NASA TECHNICAL MEMORANDUM

NASA TM X-3263

NASA TM X-3263

ACOUSTIC CHARACTERISTICS OF A LARGE-SCALE WIND-TUNNEL MODEL OF A JET FLAP AIRCRAFT

Michael D. Falarski, Thomas N. Aiken, and Kiyoshi Aoyagi

Ames Research Center
and U.S. Army Air Mobility R&D Laboratory
Moffett Field, Calif. 94035

NATIONAL AERONAUTICS AND SPACE ADMINISTRATION • WASHINGTON, D. C. • JULY 1975

1. Report No.	2. Government Accession No.	3. Recipient's Catalog No.
NASA TM X-3263		

4. Title and Subtitle	5. Report Date
ACOUSTIC CHARACTERISTICS OF A LARGE-SCALE WIND-TUNNEL MODEL OF A JET FLAP AIRCRAFT	July 1975
	6. Performing Organization Code

7. Author(s)	8. Performing Organization Report No.
Michael D. Falarski, Thomas N. Aiken, and Kiyoshi Aoyagi	A-5923
	10. Work Unit No. 760-61-02

9. Performing Organization Name and Address	11. Contract or Grant No.
Ames Research Center and U. S. Army Air Mobility R&D Laboratory Moffett Field, Calif. 94035	
	13. Type of Report and Period Covered Technical Memorandum
12. Sponsoring Agency Name and Address National Aeronautics and Space Administration Washington, D. C. 20546	14. Sponsoring Agency Code

15. Supplementary Notes

16. Abstract

The expanding-duct jet flap (EJF) concept is being studied as a means to attain STOL performance in turbofan-powered aircraft. The concept is a derivative of the basic jet flap with flap trailing edge blowing. The EJF attempts to solve the problem of ducting the required volume of air into the wing by providing an expanding cavity between the upper and lower surfaces of the flap. The blowing system consists of the trailing-edge main jet and a *BLC* slot at the flap knee. A short chord, control flap is available at the main flap trailing edge. This report presents the results of an investigation of the acoustic characteristics of the EJF concept on a large-scale aircraft model powered by JT15D engines.

The noise of the EJF is generated by acoustic dipoles as shown by the sixth power dependence of the noise on jet velocity. These sources result from the interaction of the flow turbulence with flap surfaces. They are probably some combination of flow interaction with the flap internal and external surfaces and the trailing edges.

Increasing the trailing edge jet from 70 percent span to 100 percent span increased the noise 2 dB for the equivalent nozzle area. Blowing at the knee of the flap rather than the trailing edge reduced the noise 5 to 10 dB by displacing the jet from the trailing edge and providing shielding from high-frequency noise.

Deflecting the flap and varying the angle of attack modified the directivity of the underwing noise but did not affect the peak noise. A forward speed of 33.5 m/sec (110 ft/sec) reduced the dipole noise less than 1 dB.

17. Key Words (Suggested by Author(s))	18. Distribution Statement
STOL Powered lift Jet flap Noise	Unclassified - Unlimited STAR Category - 07

19. Security Classif. (of this report)	20. Security Classif. (of this page)	21. No. of Pages	22. Price*
Unclassified	Unclassified	36	$3.75

*For sale by the National Technical Information Service, Springfield, Virginia 22151

NOTATION

b	wing span, m (ft)
BLC	boundary-layer control
c	wing chord (streamwise), m (ft)
h	blowing nozzle slot height, cm (in.)
L	distance from main jet exit to trailing edge, m (ft)
PNL	perceived noise level, *PNdB* ref. 2×10 N/m^2 (0.0002 microbar)
q	free-stream dynamic pressure, N/m^2 (lb/ft^2)
S/L	sideline
SPL	sound pressure level, dB ref. 2×10^{-5} N/m^2 (0.0002 microbar)
t	airfoil thickness, m (ft)
T. E.	trailing edge
U/W	underwing
V_{J_I}	isentropic velocity of main jet, m/sec (ft/sec)
V_∞	free-stream velocity, m/sec (ft/sec)
y	spanwise station, m (ft)
α	model angle of attack, deg
δ_α	aileron deflection, positive with trailing edge down, deg
δ_c	control flap deflection, positive with trailing edge down, deg; see fig. 2(d).
δ_f	flap deflection, positive with trailing edge down, deg; see fig. 2(d).
η	spanwise position, $\frac{2y}{b}$

ACOUSTIC CHARACTERISTICS OF A LARGE-SCALE WIND-TUNNEL MODEL OF A JET FLAP AIRCRAFT

Michael D. Falarski, Thomas N. Aiken, and Kiyoshi Aoyagi

Ames Research Center
and
U. S. Army Air Mobility R&D Laboratory

SUMMARY

The expanding-duct jet flap (EJF) concept is being studied as a means to attain STOL performance in turbofan-powered aircraft. The concept is a derivative of the basic jet flap with flap trailing edge blowing. The EJF attempts to solve the problem of ducting the required volume of air into the wing by providing an expanding cavity between the upper and lower surfaces of the flap. The blowing system consists of the trailing-edge main jet and a *BLC* slot at the flap knee. A short chord, control flap is available at the main flap trailing edge. This report presents the results of an investigation of the acoustic characteristics of the EJF concept on a large-scale aircraft model powered by JT15D engines.

The noise of the EJF is generated by acoustic dipoles as shown by the sixth power dependence of the noise on jet velocity. These sources result from the interaction of the flow turbulence with flap surfaces. They are probably some combination of flow interaction with the flap internal and external surfaces and the trailing edges.

Increasing the trailing edge jet from 70 percent span to 100 percent span increased the noise 2 dB for the equivalent nozzle area. Blowing at the knee of the flap rather than the trailing edge reduced the noise 5 to 10 dB by displacing the jet from the trailing edge and providing shielding from high-frequency noise.

Deflecting the flap and varying the angle of attack modified the directivity of the underwing noise but did not affect the peak noise. A forward speed of 33.5 m/sec (110 ft/sec) reduced the dipole noise less than 1 dB.

INTRODUCTION

The expanding-duct jet flap (EJF) concept is being studied as a means to attain STOL performance in turbofan-powered aircraft. The concept is a derivative of a basic jet flap and has the principal jet located at the flap trailing edge. Integrating the jet flap into high wing-loading aircraft

has been difficult because of the problem of providing sufficient duct area needed for high thrust from the wing jet. The EJF attempts to solve this problem by forming a cavity with the lower surface of the expanding flap, the wing rear span, and the upper surface of the flap system. The resulting cavity increases with flap deflection and is used to duct compressor air to the blowing system. The blowing system consists primarily of the main jet at the flap trailing edge and a *BLC* slot at the flap knee. In addition, a short chord control flap is available at the main flap trailing edge to provide additional deflection of the main jet. There is a *BLC* slot at the knee of the control flap.

A large-scale model was built and tested in the Ames 40- by 80-Foot Wind Tunnel to determine the acoustic and aerodynamics characteristics of the expandable-duct jet flap concept. The flap system extended either full span or 70-percent span with a blown aileron. The compressed air for the blown nozzles was provided by the fan bypass air from two turbofan engines mounted in the fuselage. This report presents the results of the acoustic investigation. The aerodynamics characteristics of the EJF are reported in reference 1.

The tests were performed in cooperation with Lockheed-Georgia Company and the Flight Dynamics Laboratory of the Department of Air Force.

MODEL AND APPARATUS

Figure 1(a) shows the model installed in the wind tunnel; figure 1(b) is a photograph of the model installed in the static test facility. The wing chord plane was approximately 6.1 m (20 ft) above the ground or wind-tunnel floor.

Basic Model

The geometric details of the model are given in figure 2 and table 1. The external dimensions of the model and a typical wing cross section are shown in figures 2(a) and 2(b), respectively. The wing planform is typical of those being proposed for STOL transports. Wing leading-edge stall was controlled with a full-span, leading-edge slat. The horizontal tail was not installed during the acoustic investigation.

Blowing System

The model was equipped with a separate blowing system for each semispan wing. The blowing system is shown schematically in figure 2(c). The compressed air to the wing was the fan bypass air of two JT15D-1 turbofan engines. The hot primary air of the turbofan was ducted out the aft end of the fuselage. The JT15D inlet and exhaust pipes were acoustically treated with lined suppressors.

Main jet– The blowing slot dimension for the main jet and the *BLC* jets are shown in figure 3. The main jet slot dimensions are controlled by the flap system lower surface trailing edge (see fig. 2(d)). The dimensions did not change with changes in control flap deflection. The overall dimension did differ for 30° and 60° flap deflection. Where the outboard 30 percent of the flap system was used as a blown aileron, the main jet slot was blocked.

BLC jets– The flap *BLC* slot was located on the knee of the upper surface of the flap (fig. 2(d)). The flap *BLC* slot was used as the blowing slot on the blown aileron. The aft *BLC* slot was located on the upper knee of the control flap (fig. 2(d)). The aft *BLC* slot was blocked on the blown aileron. The dimensions of the *BLC* slots are presented in figure 3.

TESTS

Wind Tunnel

Wind-tunnel tests were performed to document the pertinent acoustic characteristics at forward speed and angle of attack. The microphone array for these measurements is shown in figure 4(a). Bruel and Kjaer (B&K) 1.27-cm (0.5 in.) condenser microphones equipped with aerodynamically shaped nose cones were used to measure the acoustic pressure. The nose cones produce an omnidirectional response and reduced noise floor. The signal was recorded on an Ampex F1300A, 14-channel tape recorder at 30 ips and 108 KHz center-band frequency.

The acoustic characteristics of the model were investigated at flap deflections of 30° and 60° with a 100-percent span and 70-percent span main jet. Each configuration was tested over a range of forward speeds from $V_\infty = 0$ to 43 m/sec (0 to 140 ft/sec) and angle of attack from 0° to 20°. To determine the effect of jet velocity, V_{J_I} was varied from 140 to 210 m/sec (450 to 750 ft/sec).

Model Static

To determine the sideline acoustic characteristics and the wind-tunnel reverberation, the EJF model was installed in the static test facility as shown in figure 1(b). The underwing microphone array duplicated that utilized in the wind tunnel. The sideline was composed of five B&K 1.27-cm (1/2-in.) microphones mounted on 4.88 m (16 ft) stands (see fig. 4(b)). The microphones were equipped with porous, polyurethane-sponge wind screens.

Tests were performed with the main flap set to 30°, the aileron set to 30°, and the control flap set to 0°. Noise measurements were documented with the main jet exhausting over 70 and 100 percent of the wing span. A test was also conducted with the trailing-edge main jet sealed over the entire span and the main *BLC* slot increased to the combined area of the normal trailing edge and *BLC* jets. This configuration is referred to as the upper-surface jet flap (U. S.) as opposed to the trailing-edge jet flap (*T. E.*). The isentropic jet velocity was varied from 140 to 200 m/sec (450 to 700 ft/sec).

DATA REDUCTION

Wind-Tunnel Reverberation

The acoustic environment of the Ames 40- by 80-Foot Wind Tunnel has been shown to be semireverberant. Several techniques have been developed which allow the prediction of free-field noise levels from wind-tunnel acoustic measurements. These techniques and comparison with flight

data are reported in references 2 and 3. In all cases, the acoustic sources were broadband and not highly directional.

The technique developed for large acoustic sources involves the comparison of wind-tunnel and static spectra for identical model configuration and microphone arrays, assuming that spectral differences are attributable to reverberation only. Typical corrections for several microphones are shown in figure 5. They are independent of jet velocity and, when applied to other configurations, produce the comparison with static results shown in figure 6. The agreement is within ±1 dB above 80 Hz. Below 80 Hz, the spectra are influenced by background noise and therefore are unreliable. For the EJF model the reverberation corrections were derived from the difference between the frequency spectra of the static and wind tunnel tests for the 70 percent span *T. E.* configuration at a flap deflection of 30°. The final correction is an average of several jet velocities.

Wind-Tunnel Background Noise

The noise caused by operation of the wind tunnel and the flow of air over the microphone creates unwanted noise called the "background noise floor." To study the acoustics of a source in this environment, its *SPL* must be of sufficient magnitude to be distinguishable from the background. A comparison of the EJF model spectra with the wind-tunnel background spectra is presented in figure 7. Over the range of airspeeds and jet velocities investigated, the *SPL* of the EJF is at least 10 dB above the background at frequencies greater than 125 Hz. When interpreting data below this frequency, this background noise must be considered.

JT15D-1 Compressor and Exhaust Noise

The inlet and exhaust jet pipes of the JT15D-1 turbofan engines were provided with acoustic suppressors. The inlet suppressor was effective in suppressing the inlet fan tones and harmonics. The fan noise is also not present in the underwing noise which indicates that the aft fan noise was absorbed by the fuselage and wing ducting. The exhaust tail pipe suppressor was not sufficiently effective to prevent the primary core noise from dominating the spectra between 80 and 250 Hz. For high underwing and sideline angles, caution is necessary when interpreting data in this portion of the frequency spectrum. The *PNL* will also be influenced by this exhaust noise at large underwing and sideline angles.

Projection to 152.5 m (500 ft)

The acoustic data for each microphone are projected to 152.5 m (500 ft) along a ray from the assumed acoustic center shown in figure 4. The extrapolation was accomplished using Society of Automotive Engineers (SAE) procedures outlined in reference 4. These procedures consist of correction to standard day, spherical divergence, and atmospheric absorption. No corrections were applied for extra ground attenuation or ground reflections.

RESULTS AND DISCUSSION

Acoustic Mechanism

The sound pressure level of the expanding duct jet flap model varies with the sixth power of the isentropic jet velocity. As shown in figure 8, this is the case for all three configurations investigated (70 percent *T. E.* jet, 100 percent *T. E.* jet, and 70 percent U. S. jet). The sixth-power dependency is characteristic of acoustic dipoles. These sources are created by flow turbulence interacting with a surface to produce compressible pressure fluctuations that propagate at the speed of sound away from the surface. Reference 5 describes three turbulent flow regimes that generate dipole noise: (1) fluctuating lift, (2) edge source, and (3) turbulent boundary layer. These mechanism are a function of the characteristic length of the surface and the flow turbulence scale. A point source will exist when the flow turbulence scale is large with respect to the immersed body, causing the entire body force to be in phase with the fluctuating pressures. The edge dipole source is created by the sudden change in acoustic impedance at the trailing edge of a large surface. Direct radiation from the turbulent boundary layer occurs when the surface is very large in terms of wavelengths.

The EJF acoustic generation is a composite of the three dipole sources. The edge dipole noise of the EJF model was estimated by use of the empirical technique developed in reference 5. This result is shown in figure 9 compared with the other acoustic sources that contribute to the overall EJF noise. The frequency spectra from 12.5 to 250 Hz is dominated by extraneous noise from the background and jet pipes as described previously. The estimated edge noise indicates the edge sources are responsible for the noise in the midfrequency region of the spectra. A combination of all three types of dipole sources probably accounts for the noise in the spectra from 2500 Hz to 20 KHz. This noise cannot be predicted without a more complete investigation of internal duct flow.

Trailing Edge Jet Spanwise Extent

Increasing the main *T. E.* jet from 70 percent b to 100 percent b increased the *PNL* by 2*PNdB*, both under the wing and at the sideline (see fig. 10(a) and 11(a)) without significantly altering the acoustic directivity. Examination of the 1/3 octave band frequency spectra shown in figures 10(b) and 11(b)-(c) indicates the result was produced by an increase in midrange *SPL* (500 to 2500 Hz).

Upper-Surface Blowing

Blowing at the knee of the upper flap rather than the trailing edge reduced the sound pressure level from 5 to 10 dB, both under the wing and at the sideline (see figs. 12 and 13). This reduction was over the complete region of the spectra dominated by dipole noise, indicating that the change in jet location influenced several noise mechanisms. The edge noise was reduced because the jet was displaced from the flap trailing edge, thereby reducing the velocity at the trailing edge. Estimates from reference 5 indicate that the flow decay could account for a 3-4 dB reduction in the overall level for a jet with no turning. For the *T. E.* jet, the flap edge is in the potential core regime of the flow where the *SPL* varies with $(L/h)^{0.9}$. Blowing on the upper surface moves the flap edge into characteristic decay regime where the dipole noise shows a -0.94 power dependence on L/h. At underwing angles less than 96°, the reduction with upper surface blowing is from 3 to 5 dB greater

than can be expected from dipole noise reduction (see fig. 12(a)). This larger reduction may be produced by flap noise shielding. This same phenomenon creates the lower sound levels in the over-the-wing, externally blown jet flap (OTW) concept that is also being studied as a potential STOL transport (ref. 6). As with the OTW model, there is less reduction to the sideline and in the aft underwing quadrant (see figs 12(c) and 13(a)-(c)).

Main and Control Flap Deflection

Deflecting either the main flap (δ_f) or the control flap (δ_c) shifted the *PNL* directivity forward (figs. 14(a)-(b) and 15(a)-(b)). The peak *PNL* was not affected by the deflection. As expected, the directivity of the edge dipole was responsible for the *PNL* effect, as shown by the frequency spectra in figures 14(c)-(d) and 15(c)-(e) as the variation in *SPL* at high frequencies.

Acoustics at Forward Speed

Airspeed (V_∞) had only a small effect on the acoustics of the EJF. It lowered the *PNL* under the wing by less than 1 *PNdB* with no effect on directivity (figs. 16(a), (b)). The reduction with airspeed was over the entire spectra dominated by dipole noise sources (figs. 16(c) and (d)).

Varying the wing angle of attack produced a shift in the edge noise directivity (fig. 17), apparent in both the *PNL* directivity and frequency spectra.

CONCLUDING REMARKS

The expanding-duct jet flap model noise shows a sixth-power dependency on jet velocity, which is characteristic of the dipole acoustic generation mechanism. Dipole noise was created in the wing and flap ducting by direct radiation from the turbulent boundary layer and by fluctuating lift generation on internal obstructions. Dipole noise was also created at the flap trailing edge by the rapid acoustic impedance variation that occurs at the edge.

The noise increased by 2 dB when the spanwise extent of the trailing edge blowing was increased from 70-percent b to 100-percent b.

Blowing on the upper surface of the flap knee rather than at the trailing edge reduced the noise by 5 to 10 dB. The edge noise was lower because it was in the characteristic decay regime of the flow rather than the potential core as is the case with the trailing-edge configuration. The high-frequency noise under the wing was also lower as a result of flap and wing acoustic shielding.

Deflecting the flap shifted the edge noise directivity but did not effect the peak *PNL*. This was also true for angle-of-attack variations.

Forward speed had little significant effect on the noise. The *PNL* was reduced less than 1 *PNdB* with no effect on its directivity.

Ames Research Center
National Aeronautics and Space Administration
Moffett Field, Calif. 94035, March 11, 1975

REFERENCES

1. Aiken, Thomas N.; Aoyagi, Kiyoshi; and Falarski, Michael D.: Aerodynamics Characteristics of a Large-Scale Model with a Swept Wing and a Jet Flap with Expandable Duct. NASA TM X-62,281, 1973.

2. Atencio, Adolph; and Soderman, Paul T.: Comparison of Aircraft Noise Characteristics Measured in Flight Tests and in the NASA Ames 40- by 80-Foot Wind Tunnel. AIAA Paper 73-1047, 1973.

3. Falarski, M. D.; Koenig, D. G.; and Soderman, P. T.: Aspects of Investigating STOL Noise Using Large-Scale Wind Tunnel Models. NASA TM X-62,164, 1972.

4. Anon: Standard Values of Atmospheric Absorption as a Function of Temperature and Humidity for Use in Evaluating Aircraft Flyover Noise. SAE ARP-866, 1964.

5. Hayden, Richard E.: Noise from Interaction of Flow with Rigid Surfaces: a Review of Current Status of Prediction Techniques. NASA CR-2126, 1972.

6. Falarski, M. D.; Aoyagi, Kiyoshi; and Koenig, D. G.: Acoustic Characteristics of a Large-Scale Wind Tunnel Model of an Upper Surface Blown Flap Transport Having Two Engines. NASA TM X-62,319, 1973.

TABLE 1.– MODEL REFERENCE DIMENSIONS

Wing:			
Area, m^2 (ft^2)		21.37	(230.0)
Aspect ratio		8.00	
Taper ratio		0.30	
Span, m (ft)		13.080	(42.895)
Root chord, m (ft)		2.510	(8.250)
Tip chord, m (ft)		0.750	(2.475)
Mean aerodynamic chord, m (ft)		1.790	(5.881)
Sweep at 1/4 chord, deg		27.5	
Airfoil section	NACA	65A - 4 XX	
	root t/c =	0.125	
	tip t/c =	0.105	
Incidence, twist		0	
Vertical Tail:			
Area, m^2 (ft^2)		6.32	(68.0)
Aspect ratio		1.20	
Taper ratio		0.74	
Span, m (ft)		2.760	(9.04)
Root chord, m (ft)		2.630	(8.65)
Tip chord, m (ft)		1.950	(6.40)
Mean aerodynamic chord, m (ft)		2.310	(7.58)
Sweep at 1/4 chord, deg		38.5	
Airfoil section	NACA	0012	
Volume coefficient		0.114	
Horizontal Tail:			
Area, m^2 (ft^2)		6.72	(72.3)
Aspect ratio		4.00	
Taper ratio		0.49	
Span, m (ft)		2.590	(8.50)
Root chord, m (ft)		1.740	(5.71)
Tip chord, m (ft)		0.850	(2.80)
Mean aerodynamic chord, m (ft)		1.350	(4.42)
Sweep at 1/4 chord, deg		25	
Airfoil section (inverted)	NACA	64-012	
Volume coefficient		1.038	

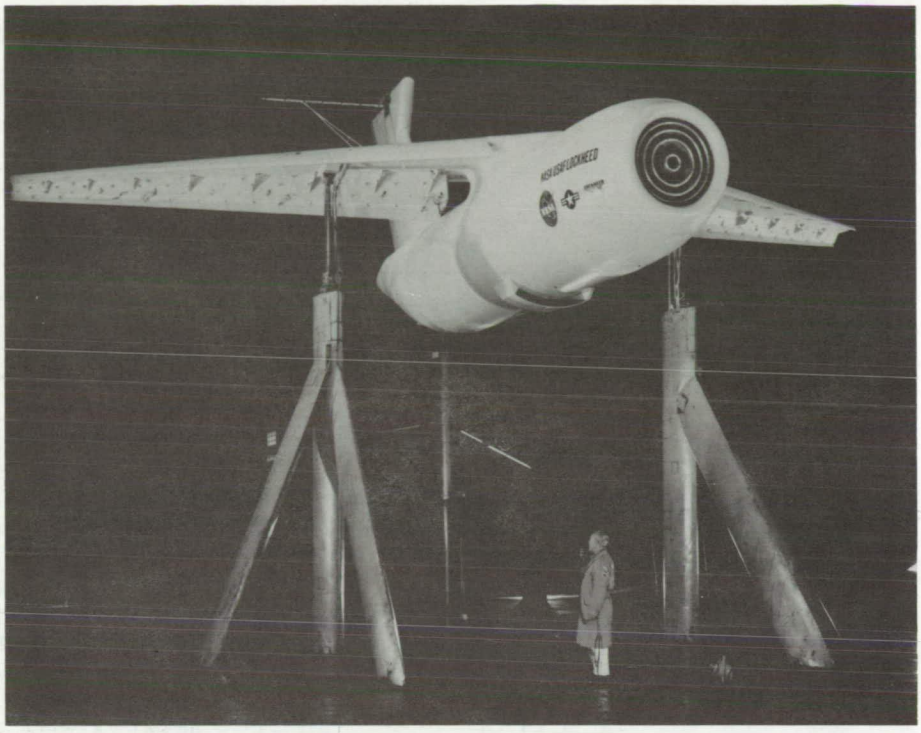

(a) Installation in wind tunnel.

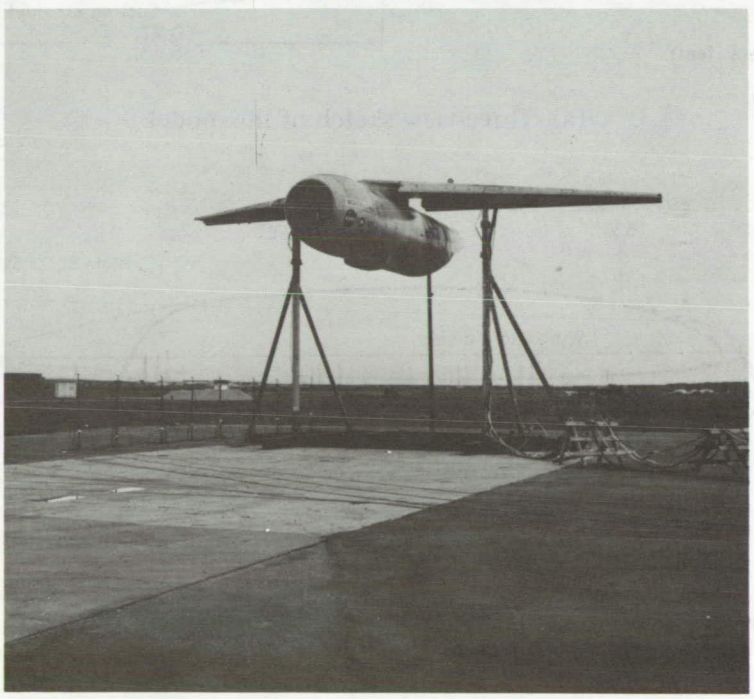

(b) Installation in static test facility.

Figure 1.– EJF model test installations.

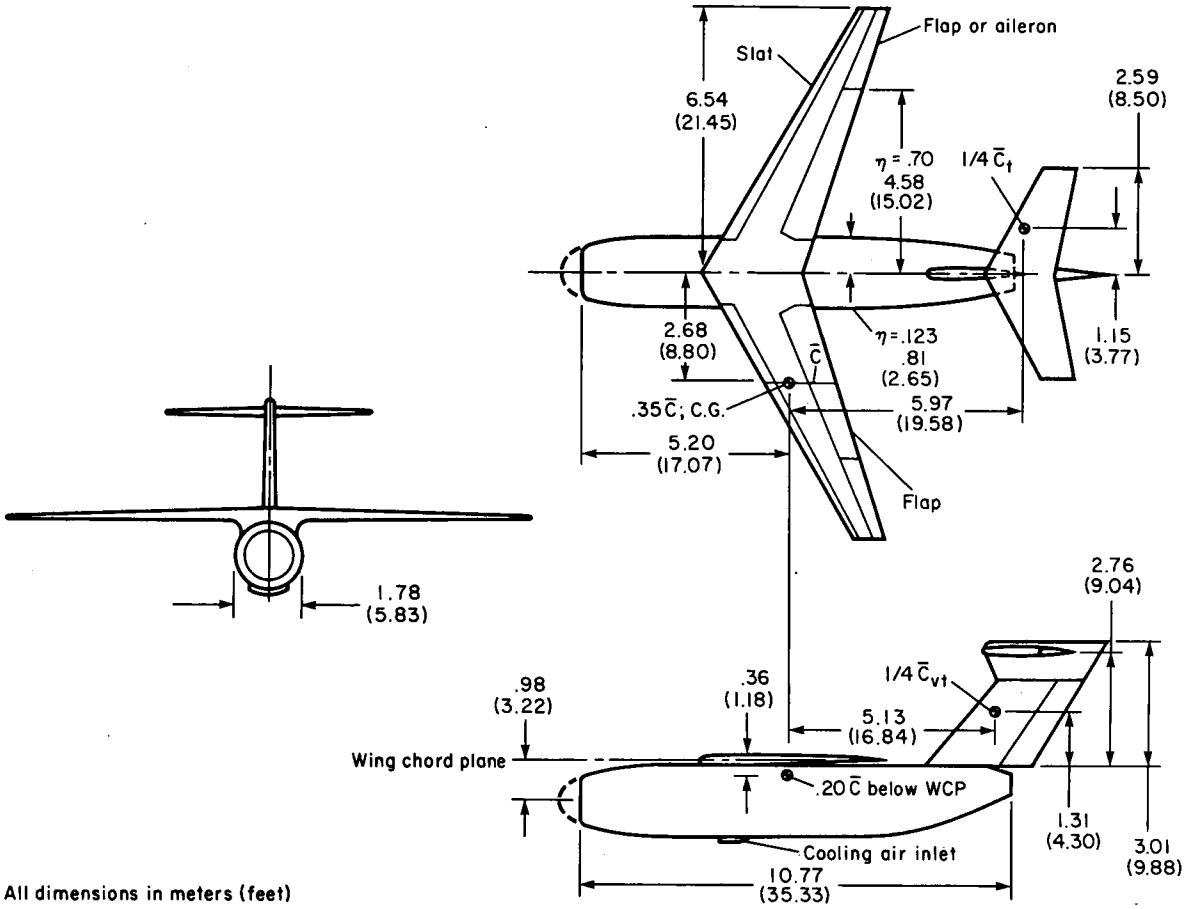

(a) Three-view sketch of the model.

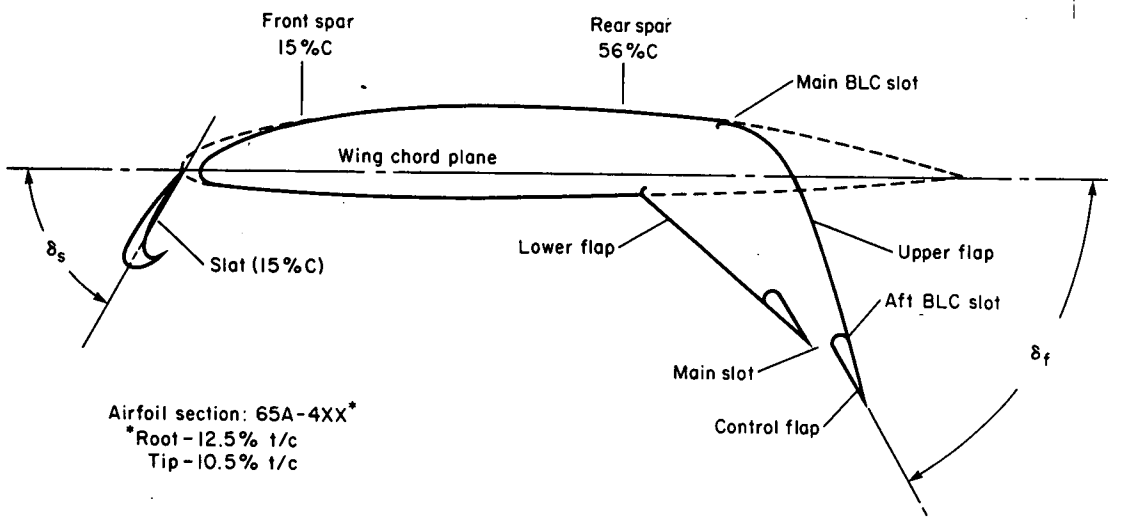

(b) Wing section geometry.

Figure 2.– Geometric details of the model.

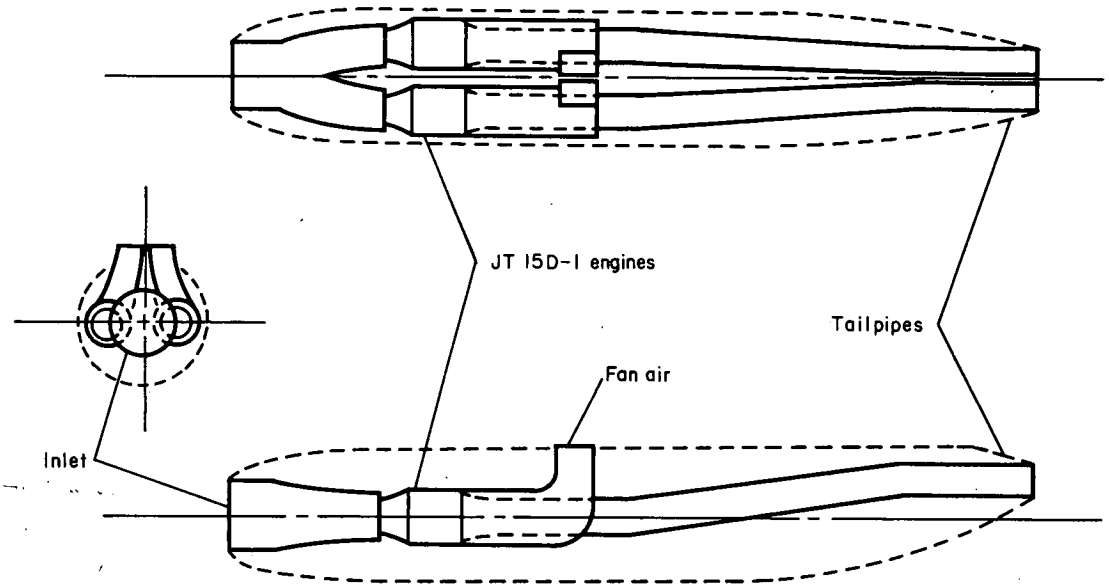

(c) Schematic of the air supply system.

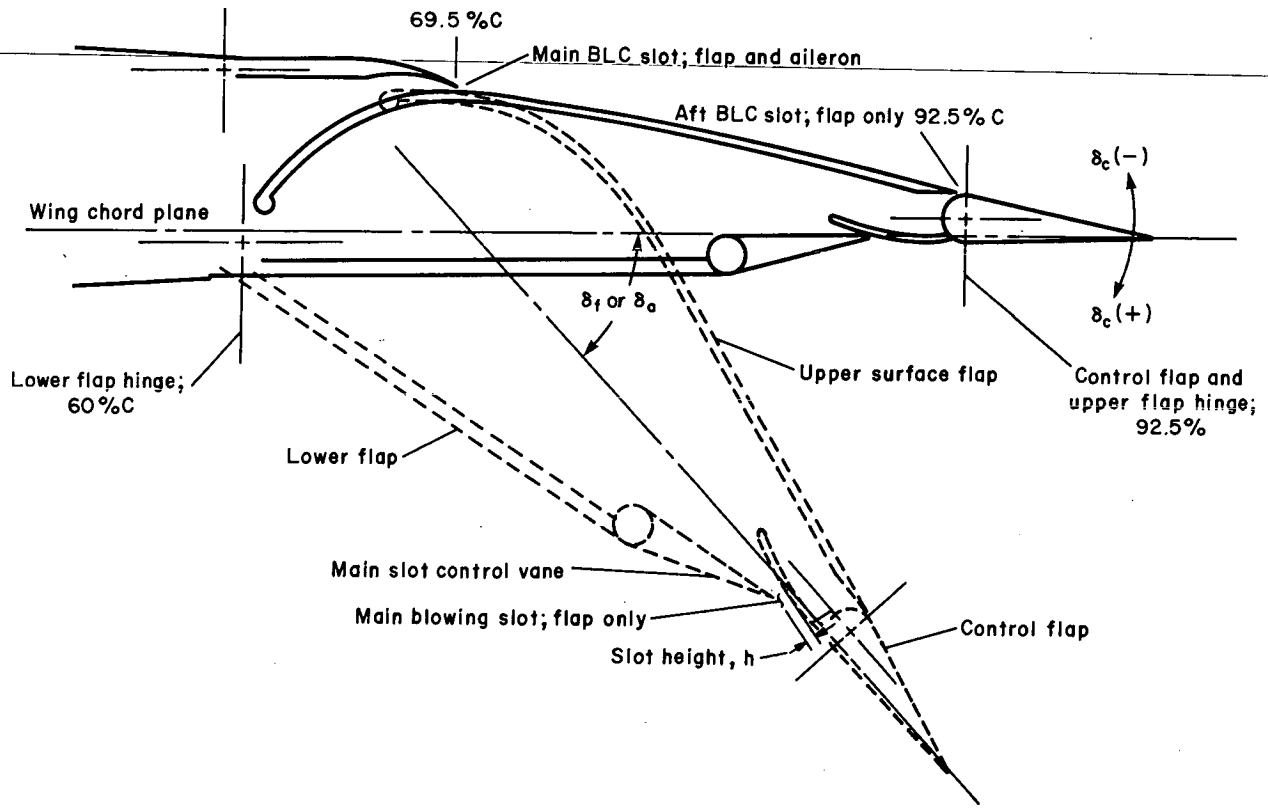

(d) Flap section geometry.

Figure 2.– Concluded.

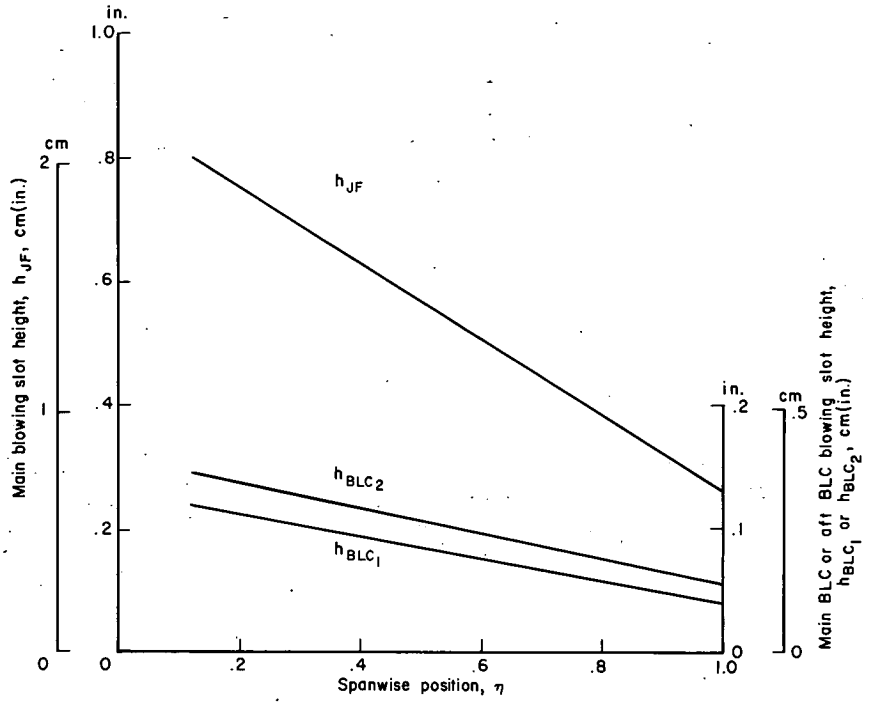

(a) $\delta_f = 60°$, full-span flap.

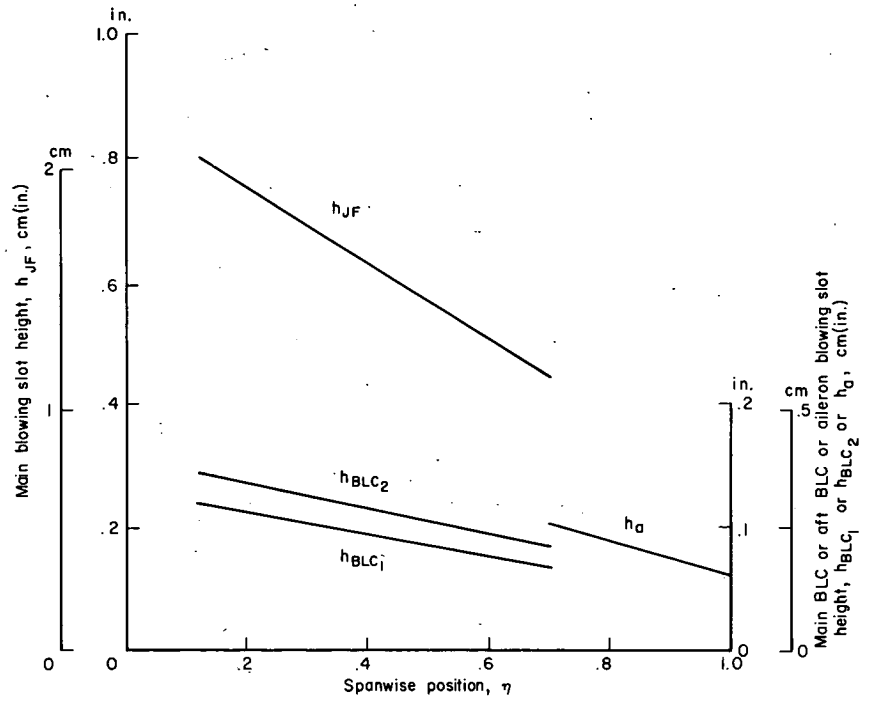

(b) $\delta_f = 60°$, partial span flap.

Figure 3.– Dimensions of model blowing slots.

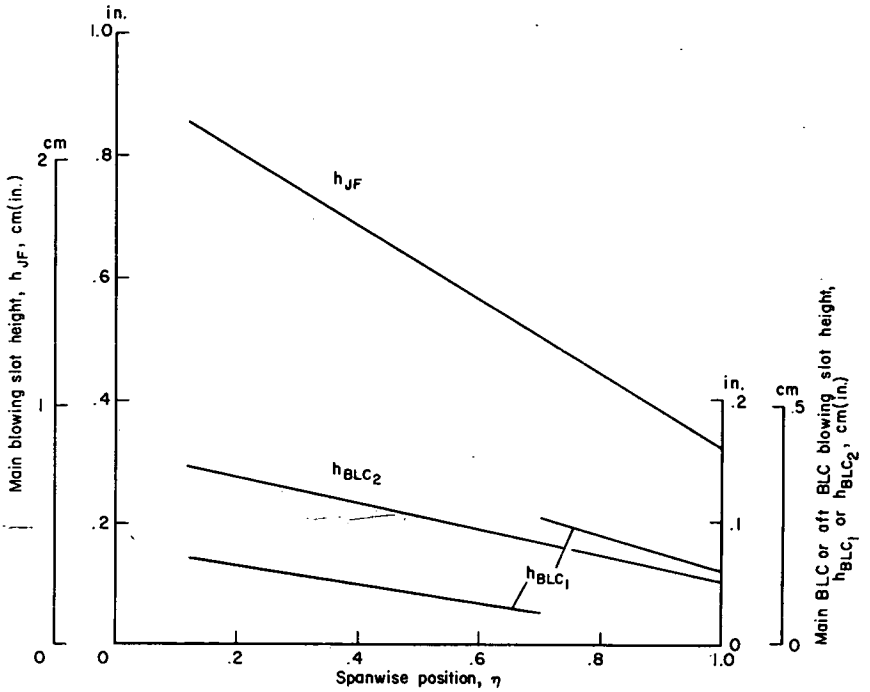

(c) $\delta_f = 30°$, full-span flap.

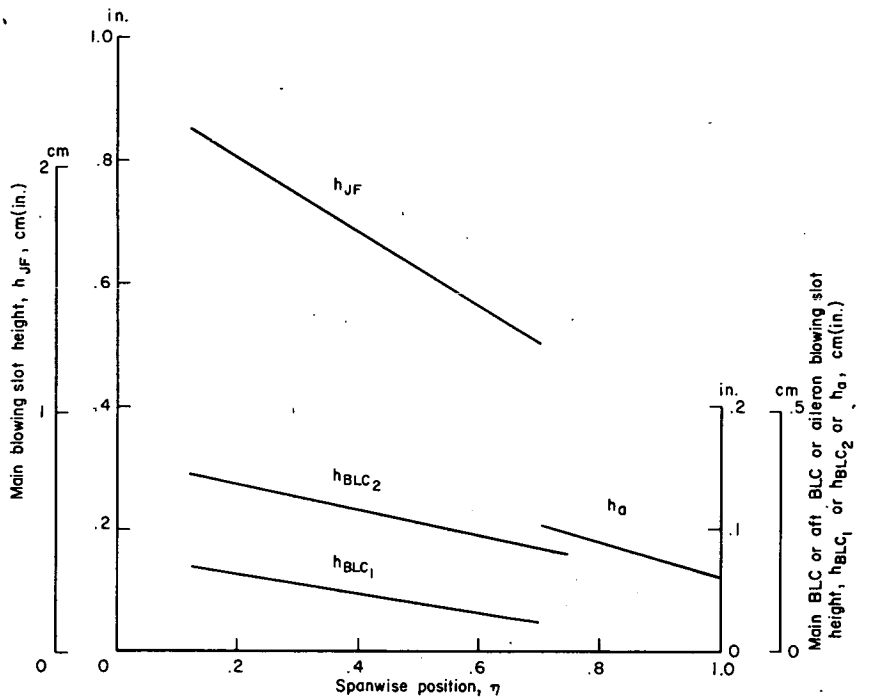

(d) $\delta_f = 30°$, partial span flap.

Figure 3.– Concluded.

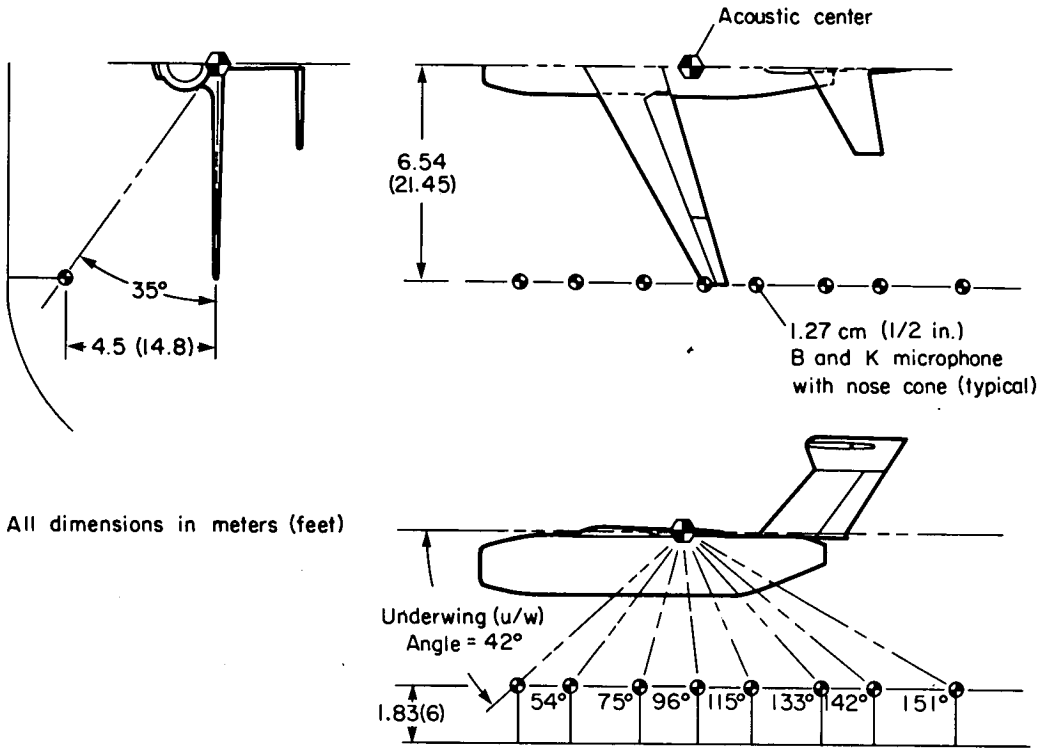

(a) Underwing microphone array.

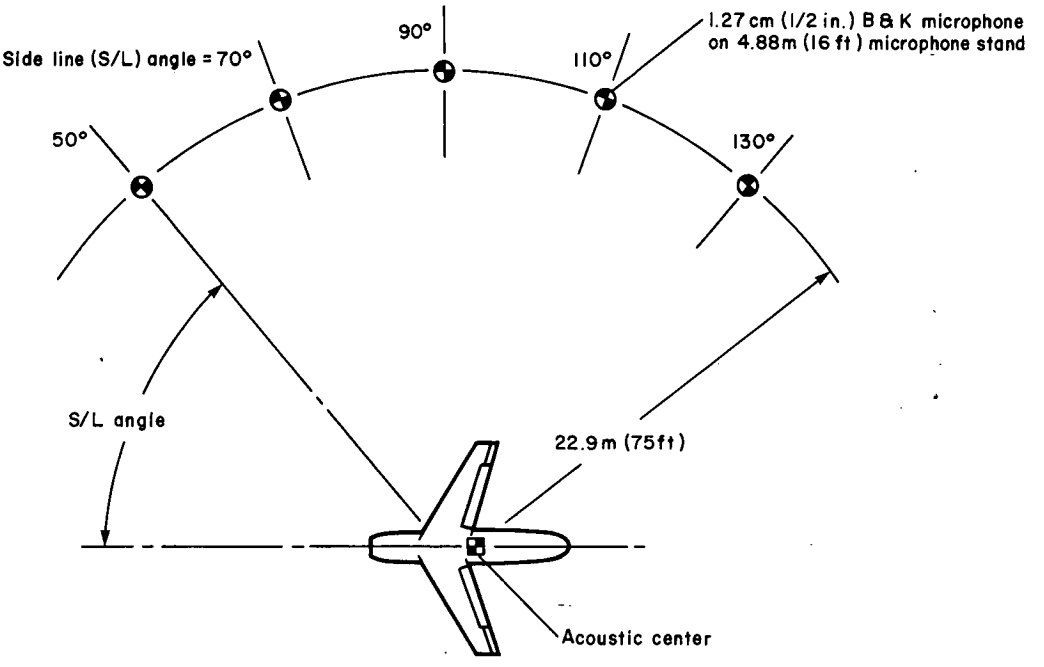

(b) Sideline microphone array.

Figure 4.– Geometric details of microphone array.

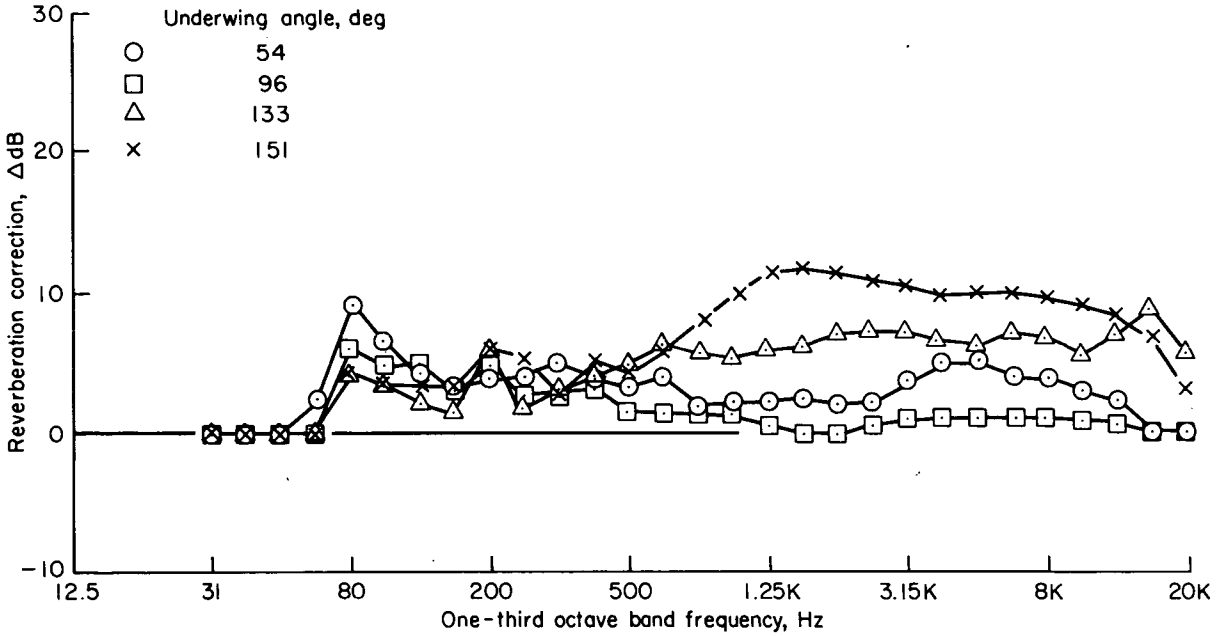

Figure 5.– Typical wind-tunnel reverberation corrections.

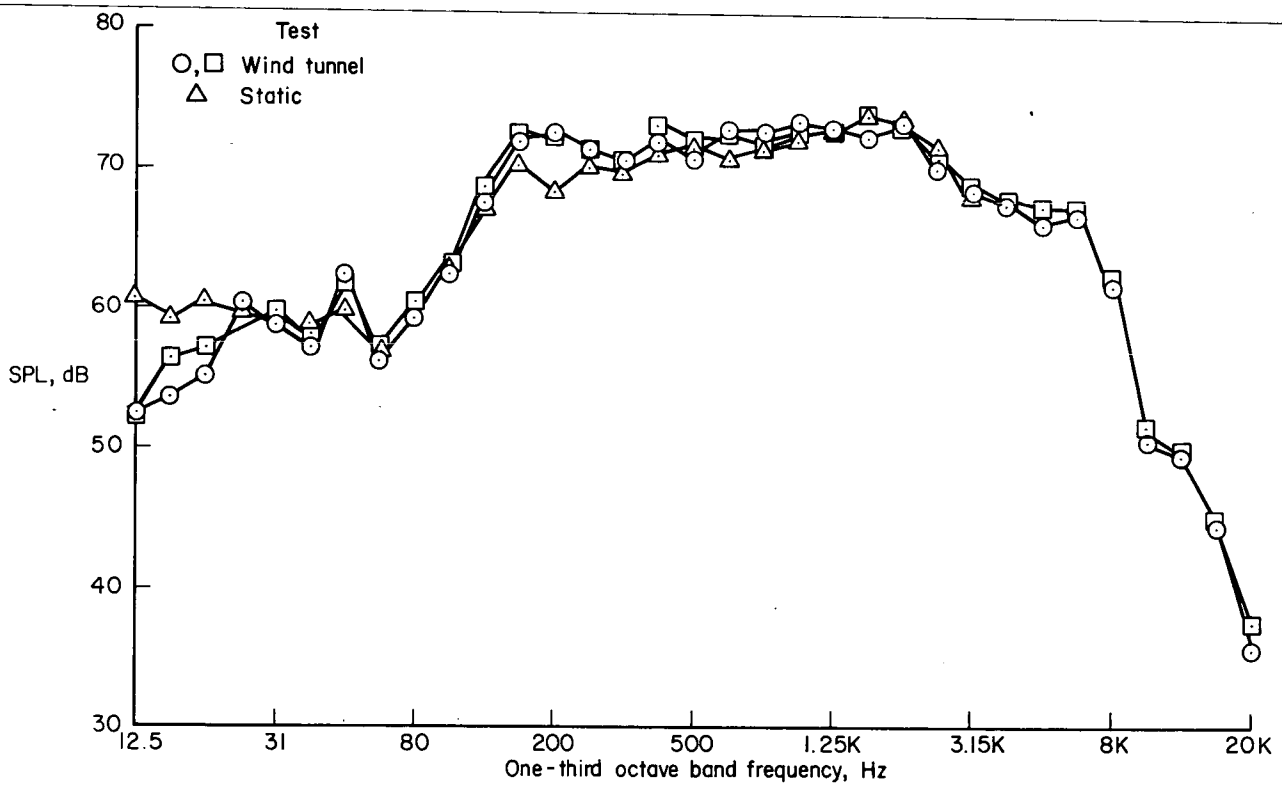

Figure 6.– Comparison of corrected wind-tunnel and static test frequency spectra; $\delta_f = 30°$, $\delta_c = 0°$, $\delta_a = 30°$, $V_{J_I} = 200$ m/sec (665 ft/sec), U/W angle = 115°, $\alpha = 0°$, $V_\infty = 0$.

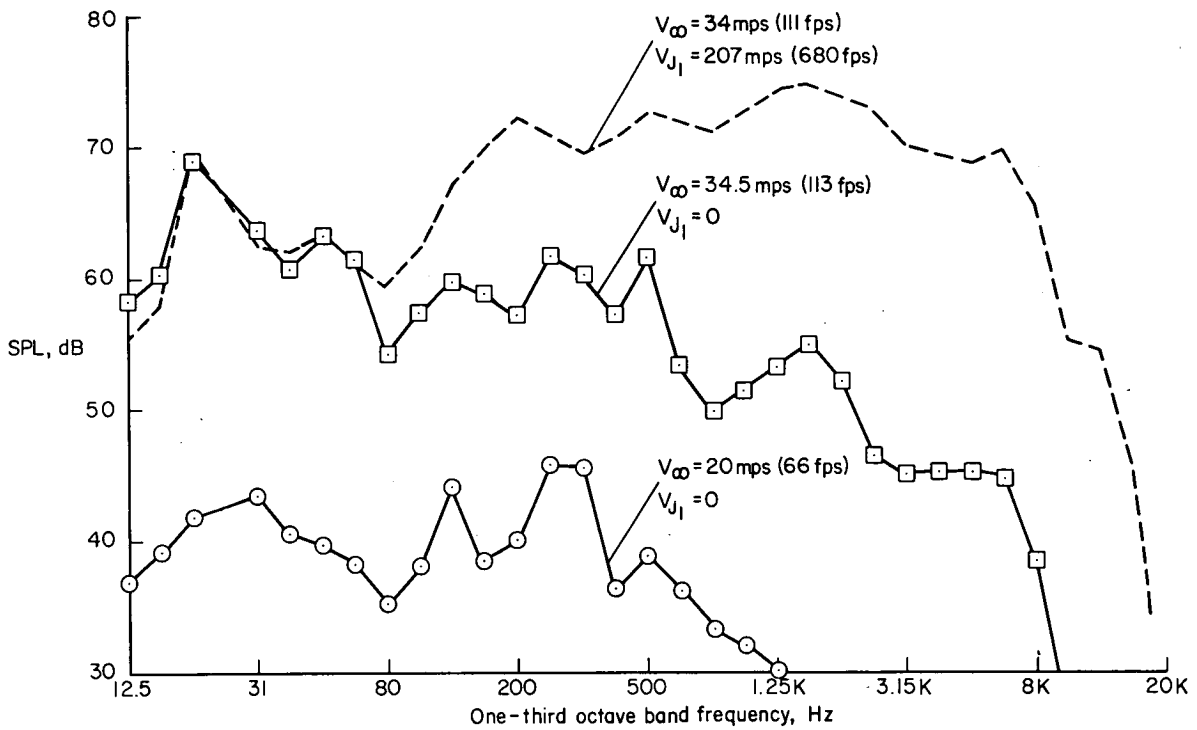

Figure 7.– Wind-tunnel background noise floor; $\delta_f = 60°$, $\delta_c = 0°$, $\delta_a = 30°$, $\alpha = 0°$, U/W angle = 96°.

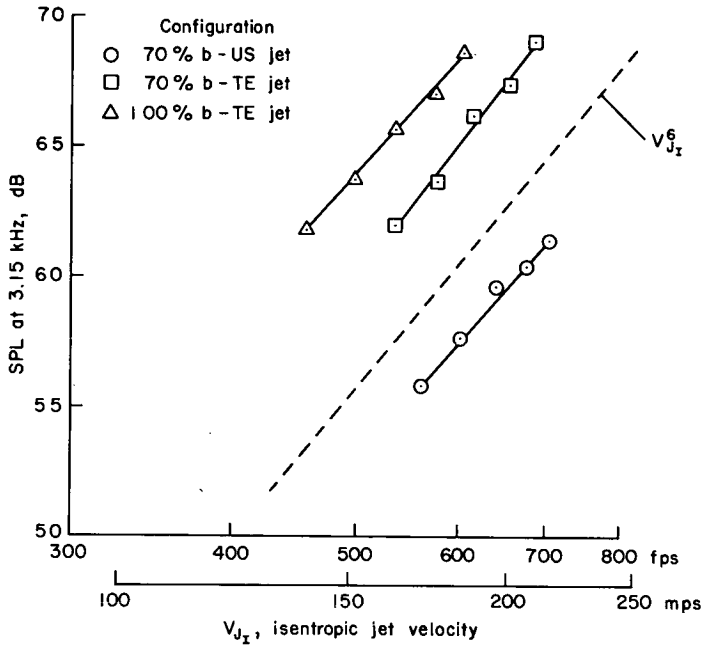

(a) Frequency = 3150 Hz.

Figure 8.– Variation of *SPL* with V_{J_I}; $\delta_f = 30°$, $\delta_c = 0°$, $\delta_a = 30°$, *U/W* angle = 115°, $\alpha = 0$.

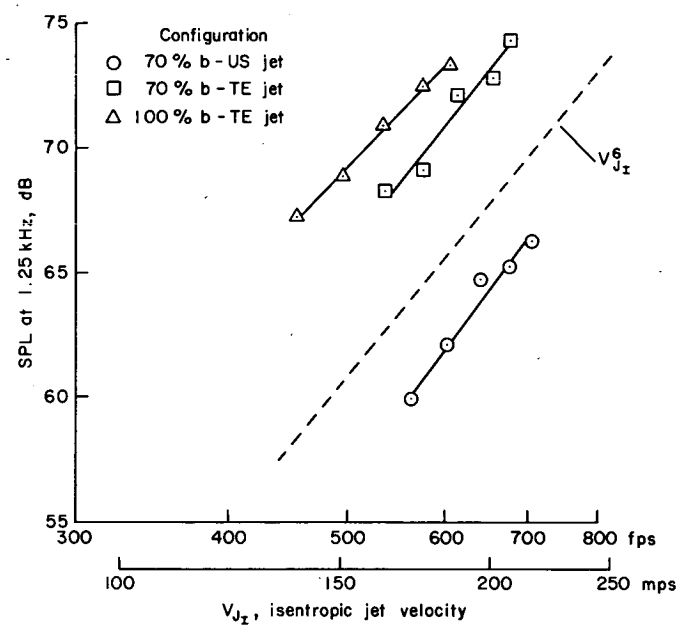

(b) Frequency = 1250 Hz.

Figure 8.– Concluded.

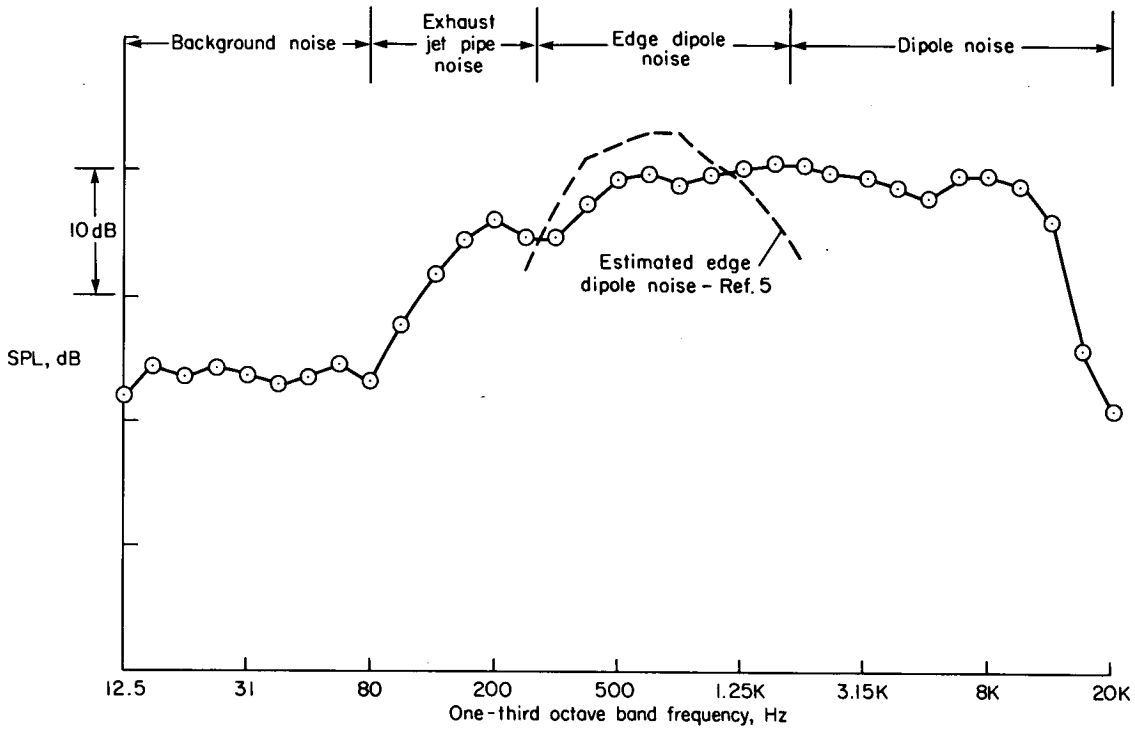

Figure 9.– EJF acoustic sources; $\delta_f = \delta_a = 30°$, $\delta_c = 0$, $V_{J_I} = 213$ m/sec (700 ft/sec), $V_\infty = \alpha = 0$, jet percent $b = 70$, U/W angle $= 75°$.

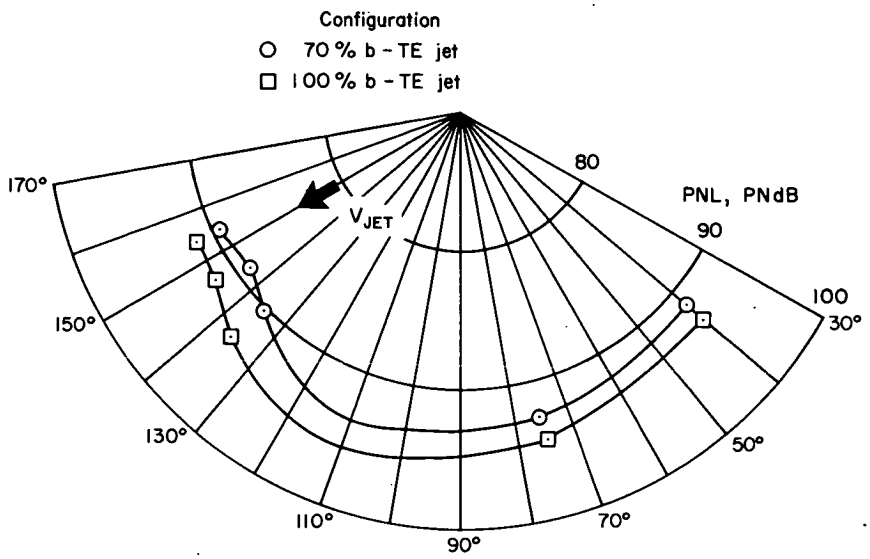

(a) *PNL* directivity.

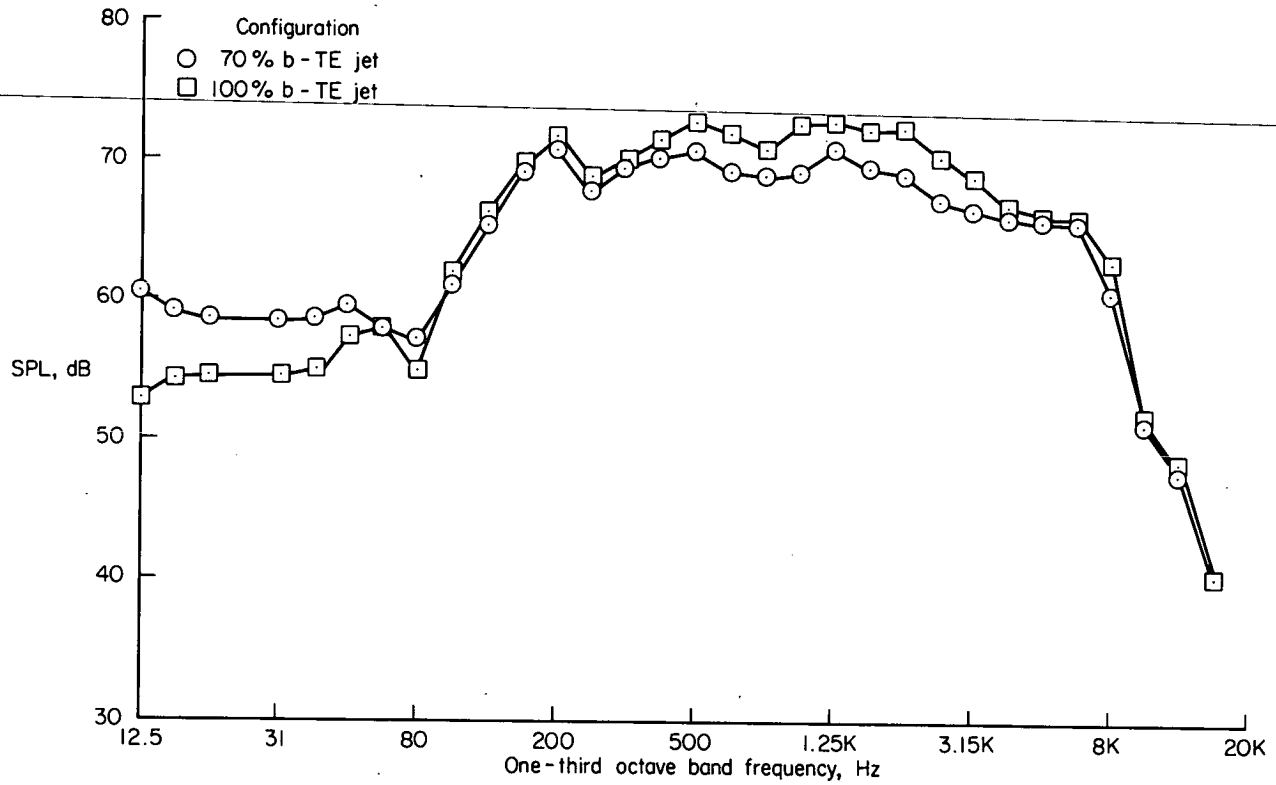

(b) Frequency spectra, U/W angle = 75°.

Figure 10.– Effect of main jet spanwise extent on EJF underwing noise; $\delta_f = \delta_a = 30°$, $\delta_c = 0$, $V_{J_I} = 186$ m/sec (610 ft/sec), $\alpha = q = 0$.

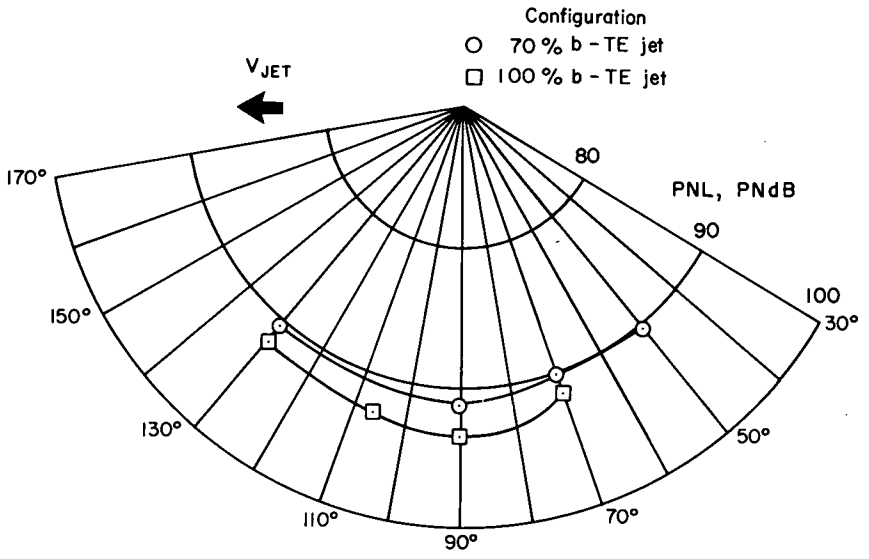

(a) *PNL* directivity.

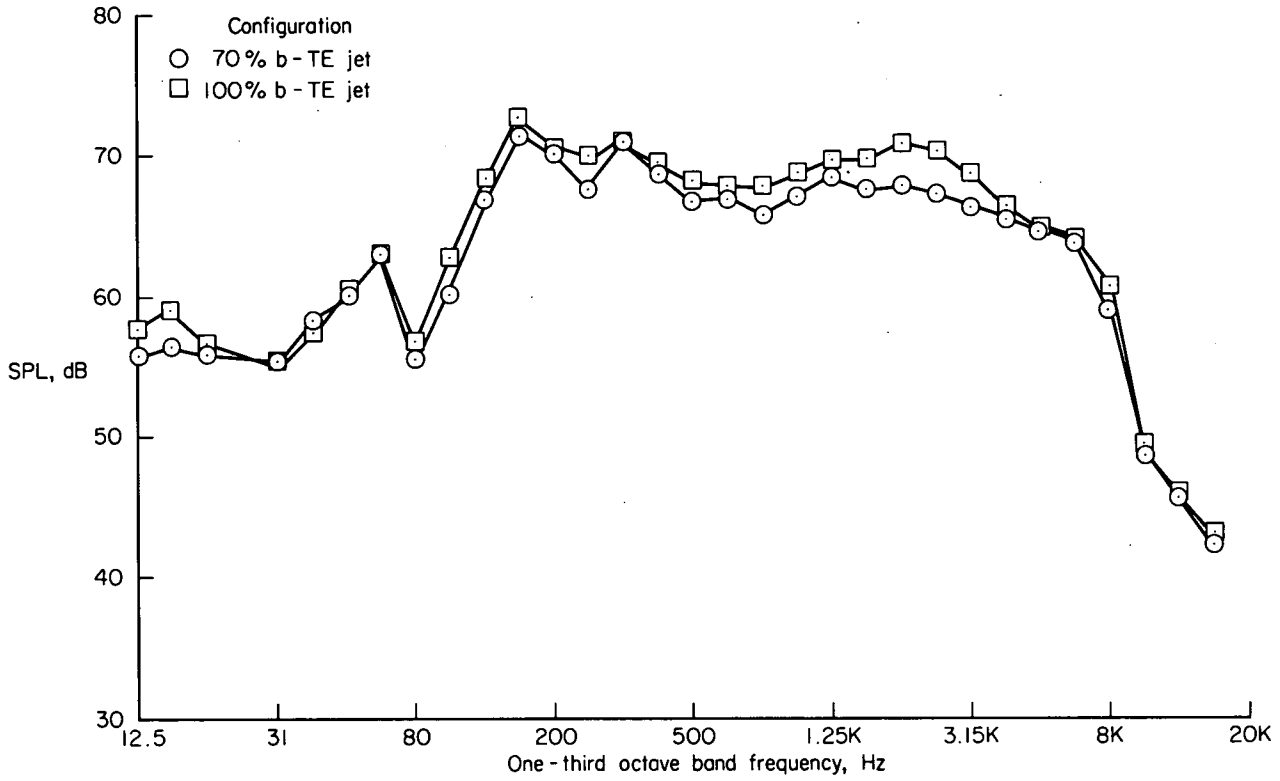

(b) Frequency spectra, S/L angle = 90°.

Figure 11.– Effect of main jet spanwise extent on EJF sideline noise; $\delta_f = 30°$, $\delta_c = 0°$, $\delta_a = 30°$, $V_{J_I} = 186$ m/sec (610 ft/sec), $\alpha = q = 0$.

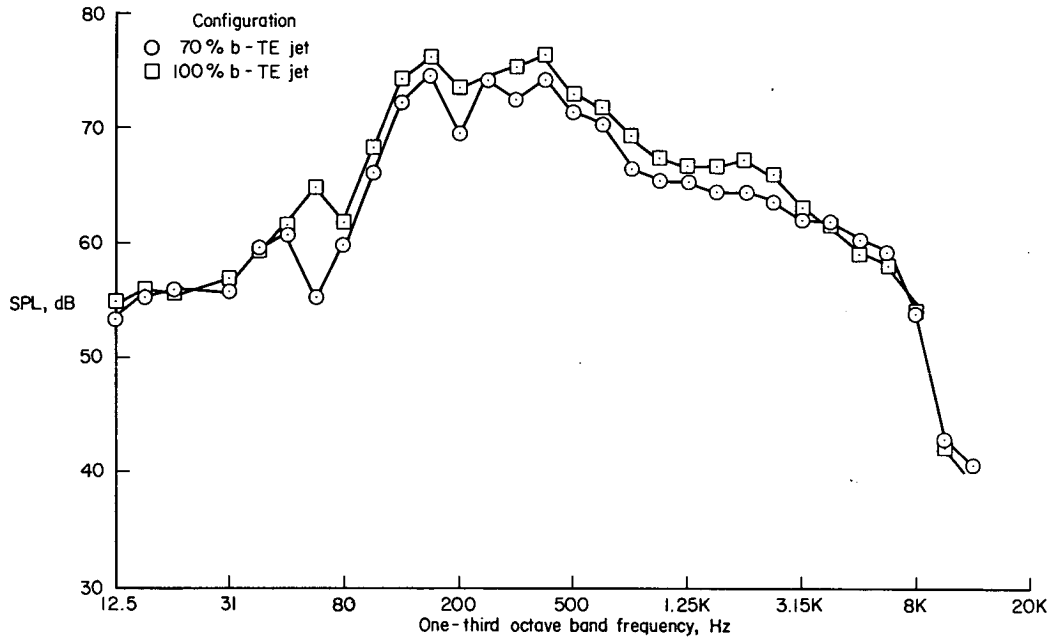

(c) Frequency spectra, S/L angle = 150°.

Figure 11.– Concluded.

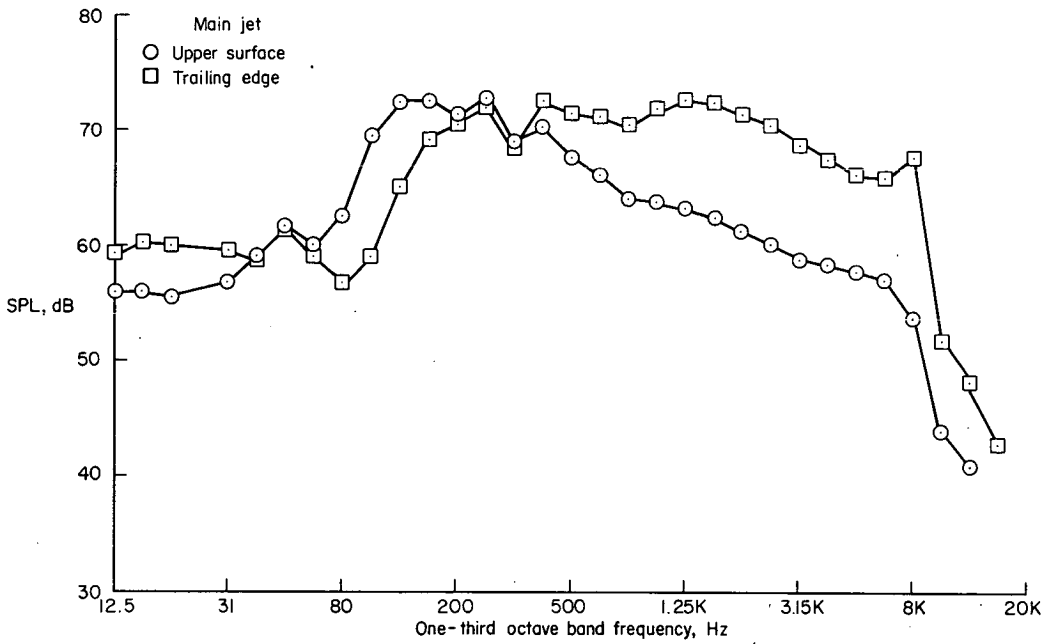

(a) U/W angle = 42°.

Figure 12.– Effect of main jet location on underwing frequency spectra; $\delta_f = 30°$, $\delta_c = 0°$, $\delta_a = 30°$, $V_{J_I} = 213$ m/sec (700 ft/sec), jet percent $b = 70$.

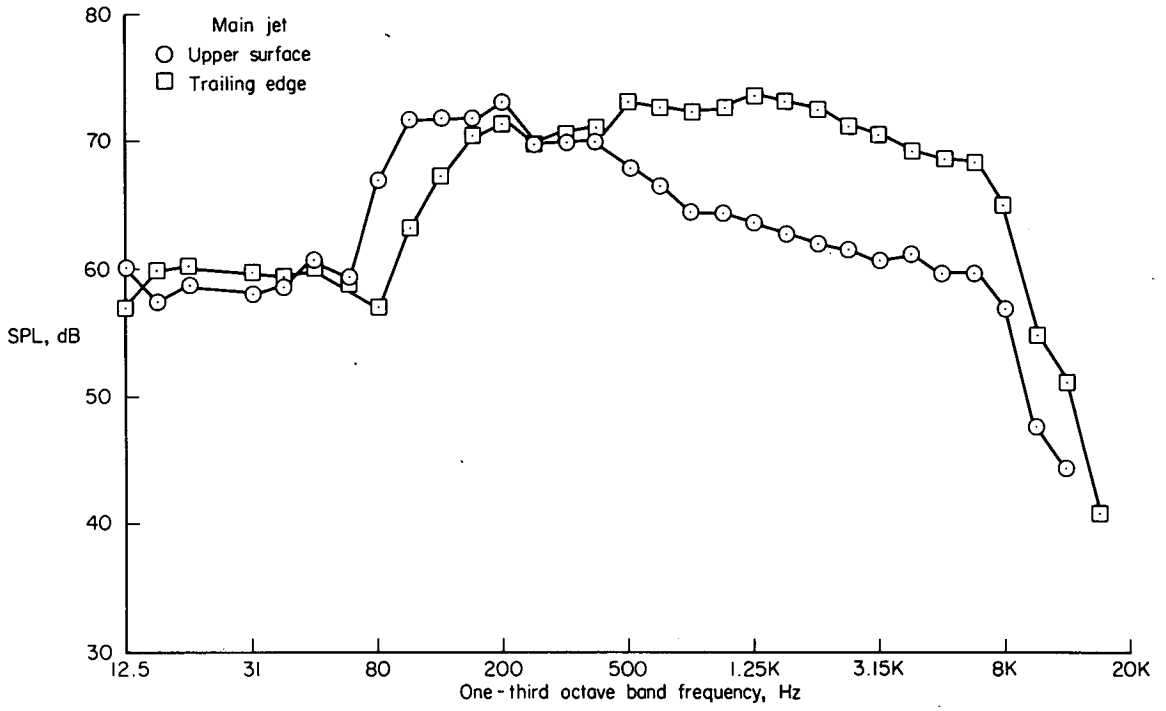

(b) U/W angle = 75°.

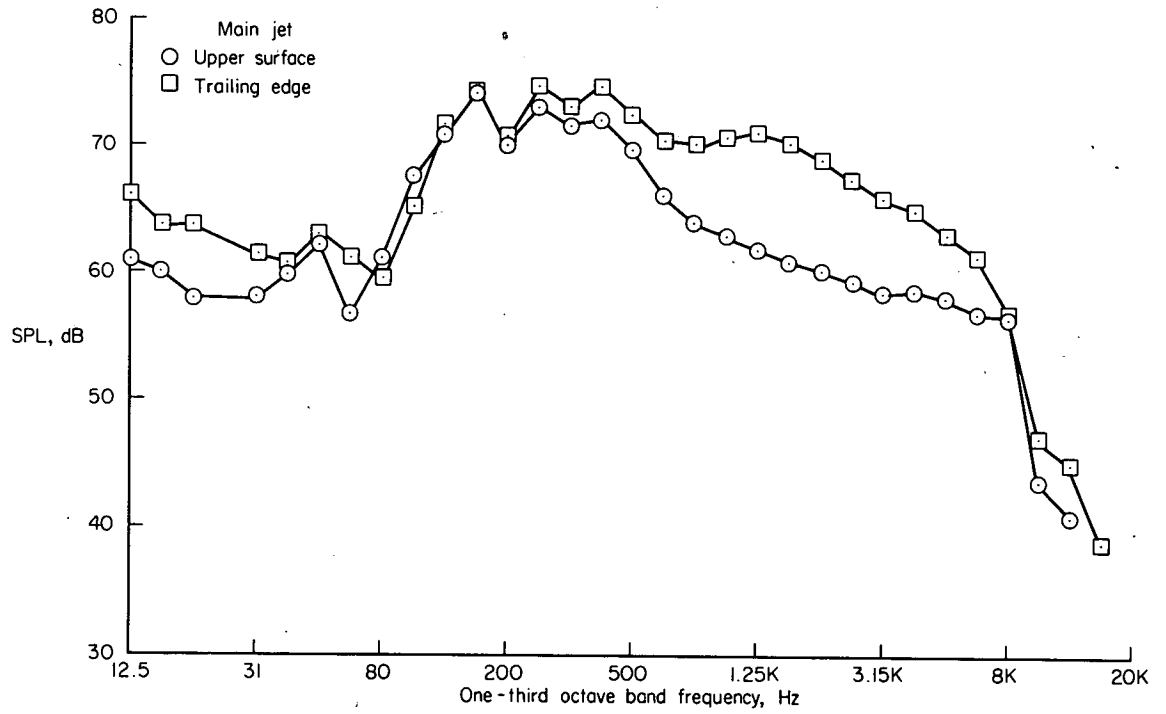

(c) U/W angle = 133°.

Figure 12.– Concluded.

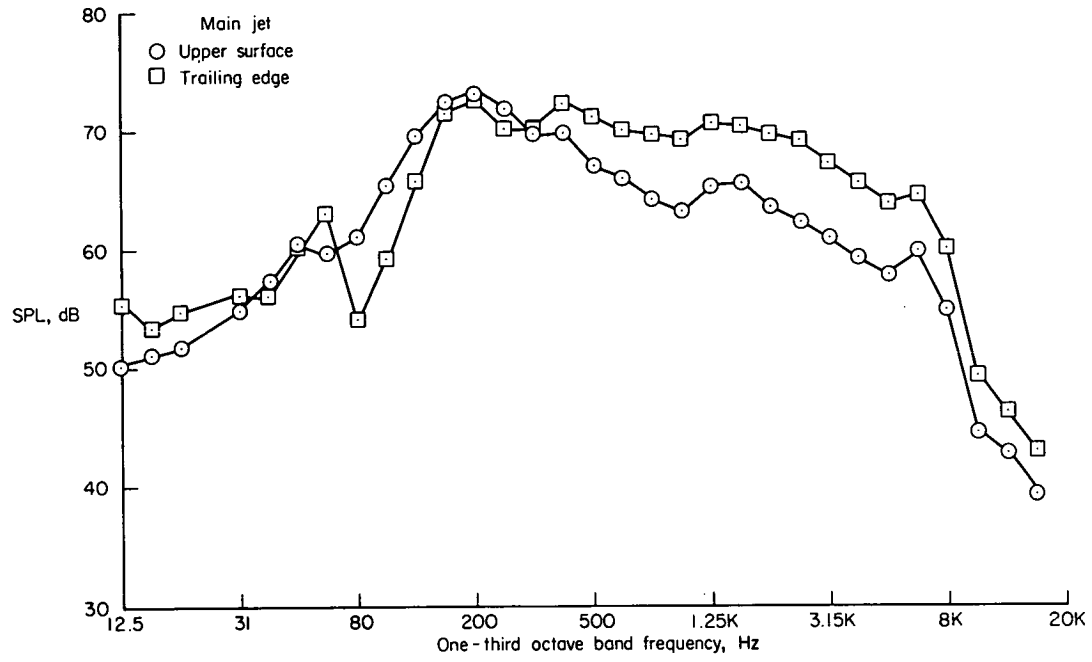

(a) S/L angle = 50°.

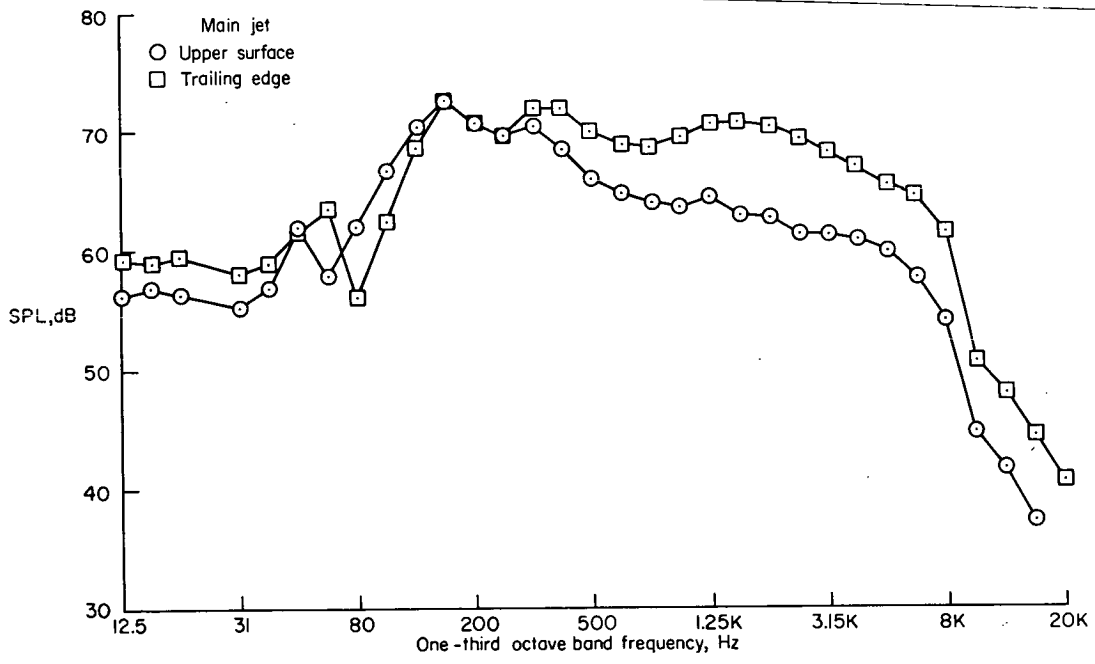

(b) S/L angle = 90°.

Figure 13.– Effect of main jet location on sideline frequency spectra; $\delta_f = 30°$, $\delta_c = 0°$, $\delta_a = 30°$. $V_{J_I} = 213$ m/sec (700 ft/sec), jet percent b =70, $\alpha = q = 0$.

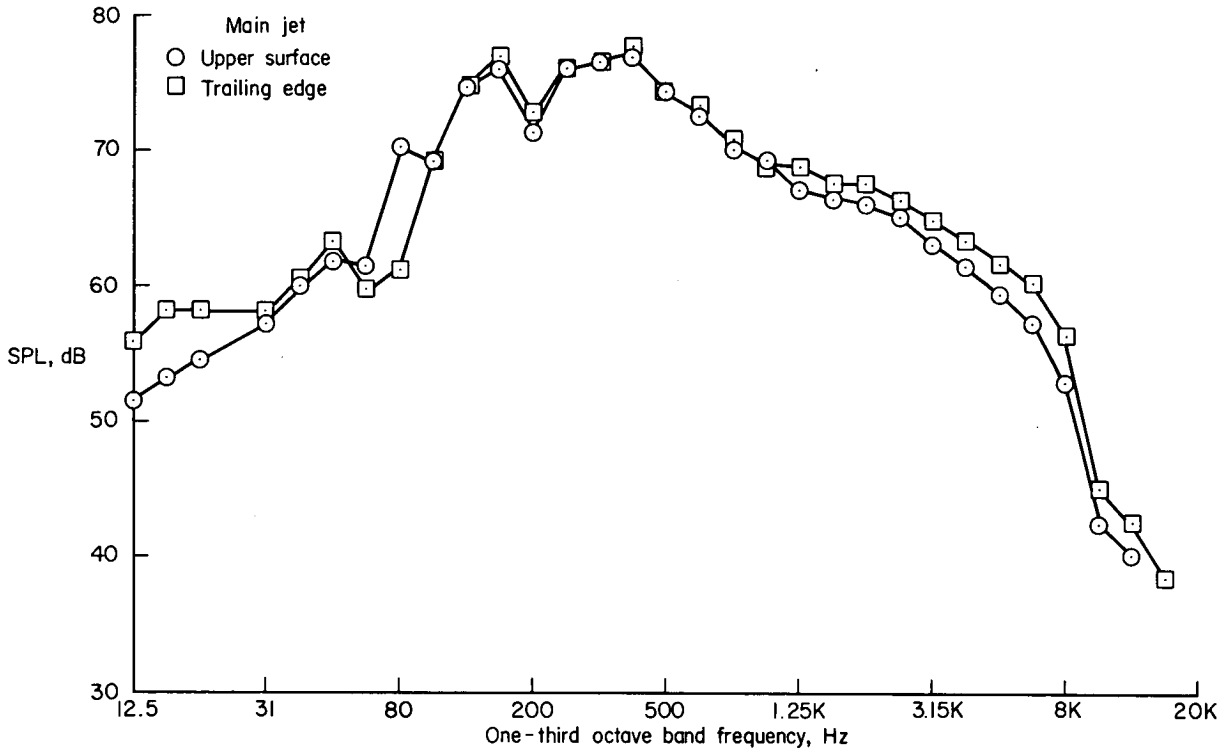

(c) S/L angle = 130°.

Figure 13.– Concluded.

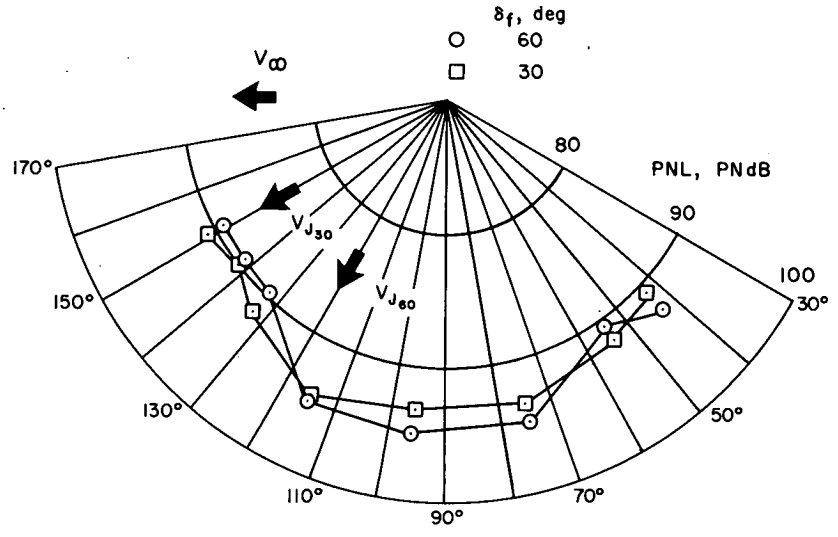

(a) *PNL* directivity, V_∞ = 38 m/sec (109 ft/sec).

Figure 14.– Variation in underwing acoustic characteristics with main flap deflection; $\delta_c = 0$, $\delta_a = 30°$, V_{J_I} = 204 m/sec (670 ft/sec), $\alpha = 0°$, jet percent $b = 70$.

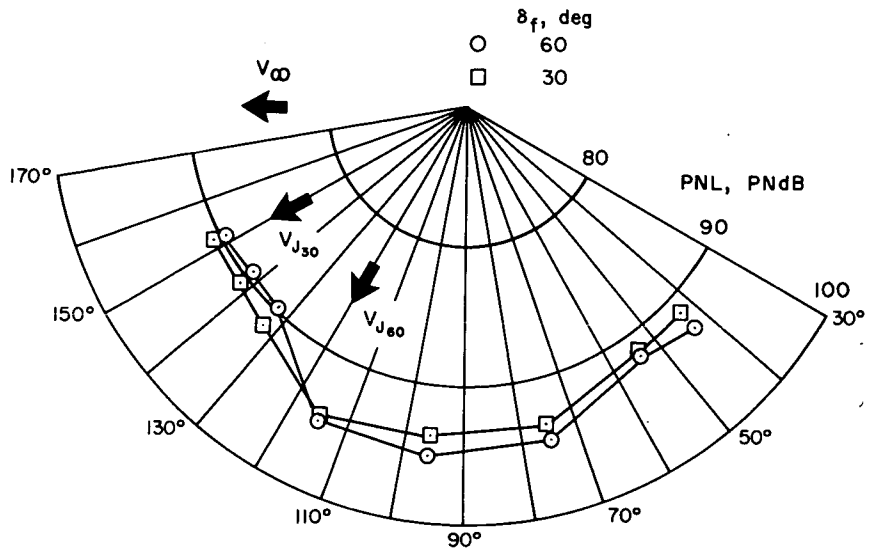

(b) *PNL* directivity, $V_\infty = 23.5$ m/sec (77 ft/sec).

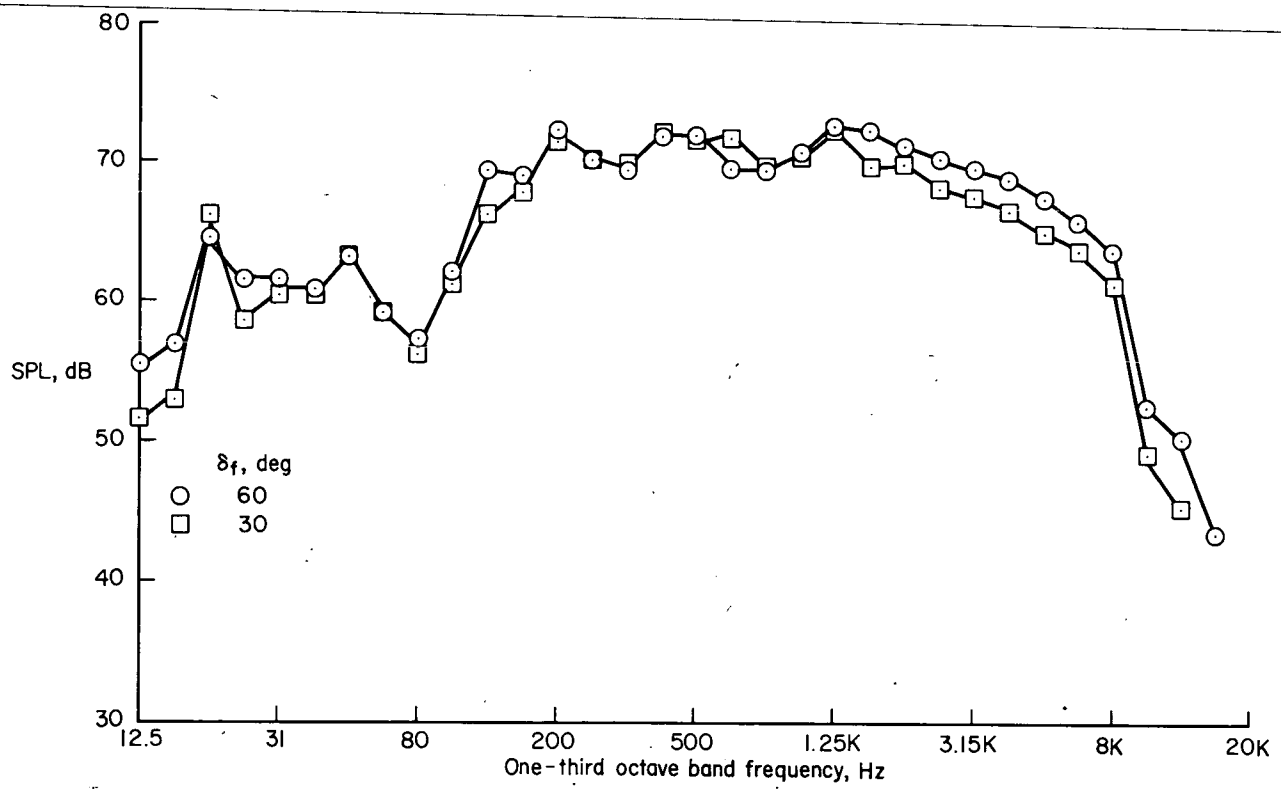

(c) Frequency spectra, U/W angle = 75°, $V_\infty = 33$ m/sec (109 ft/sec).

Figure 14.– Continued.

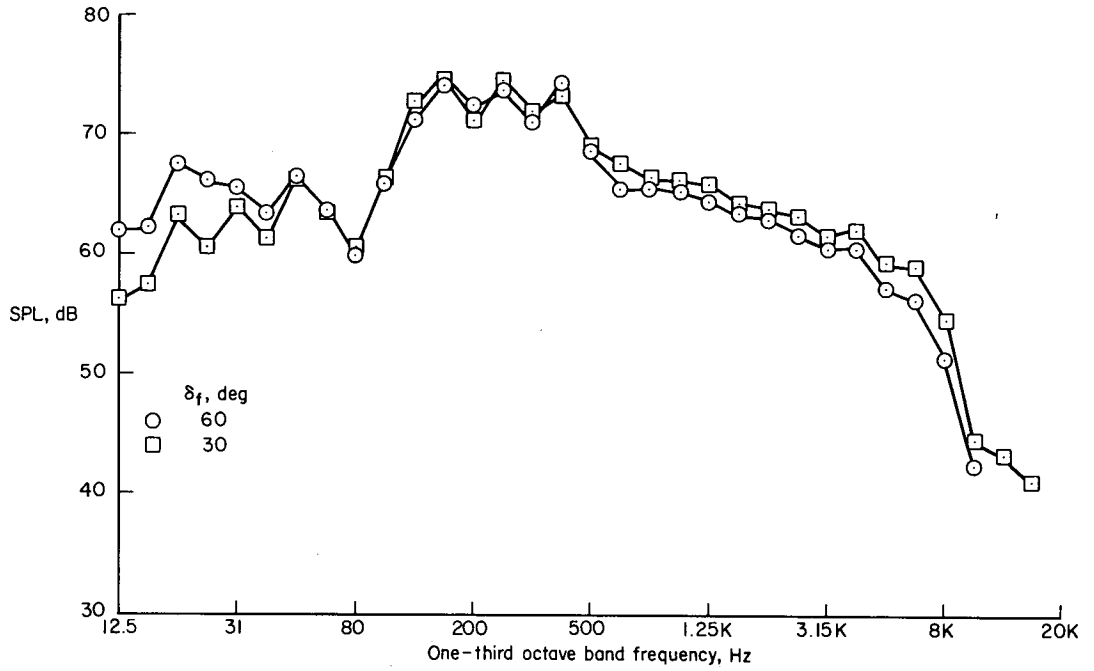

(d) Frequency spectra, U/W angle = 142°, V_∞ = 33 m/sec (109 ft/sec).

Figure 14.– Concluded.

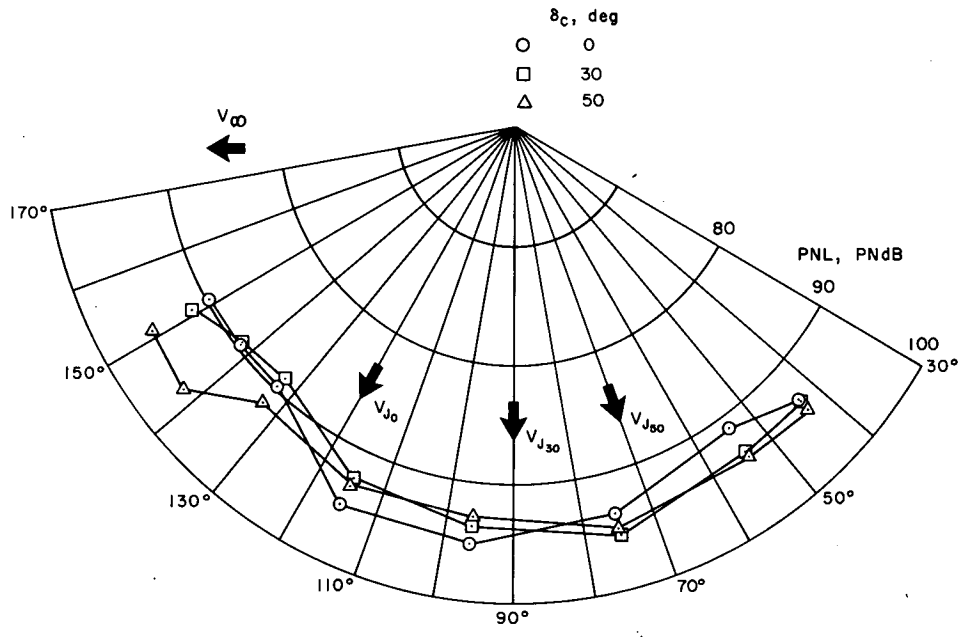

(a) *PNL* directivity, V_∞ = 19 m/sec (62 ft/sec).

Figure 15.– Variation in underwing acoustic characteristics with control flap deflection; $\delta_f = 60°$. $\delta_a = 30°$, $V_J \equiv 201$ m/sec (660 ft/sec), $\alpha = 0°$, percent $b = 70$.

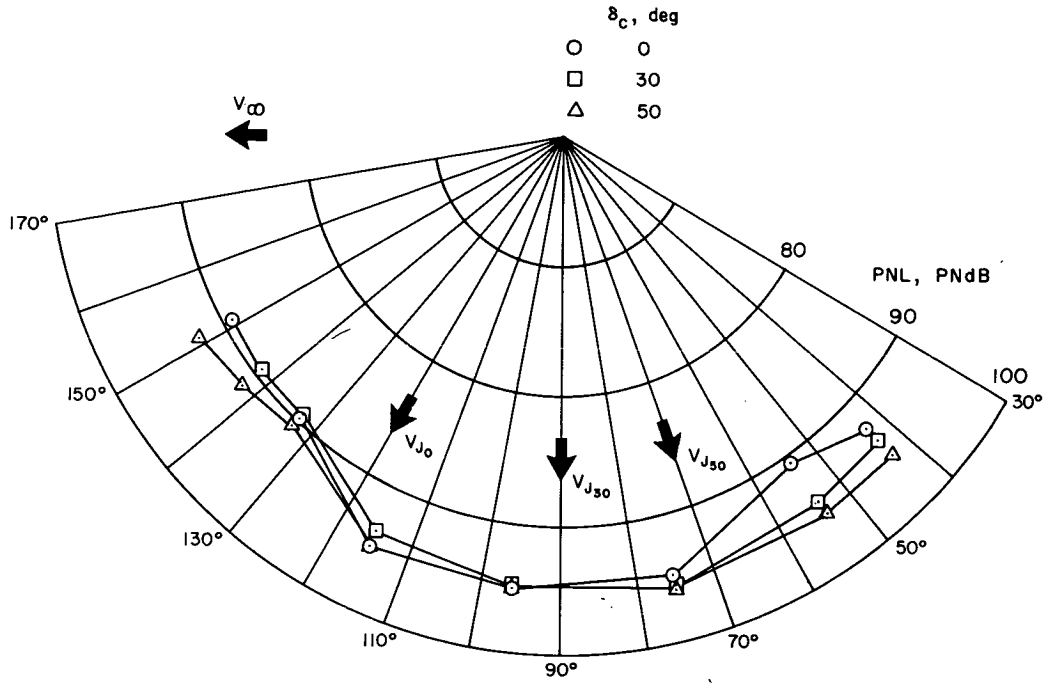

(b) *PNL* directivity, $V_\infty = 33.5$ m/sec (106 ft/sec).

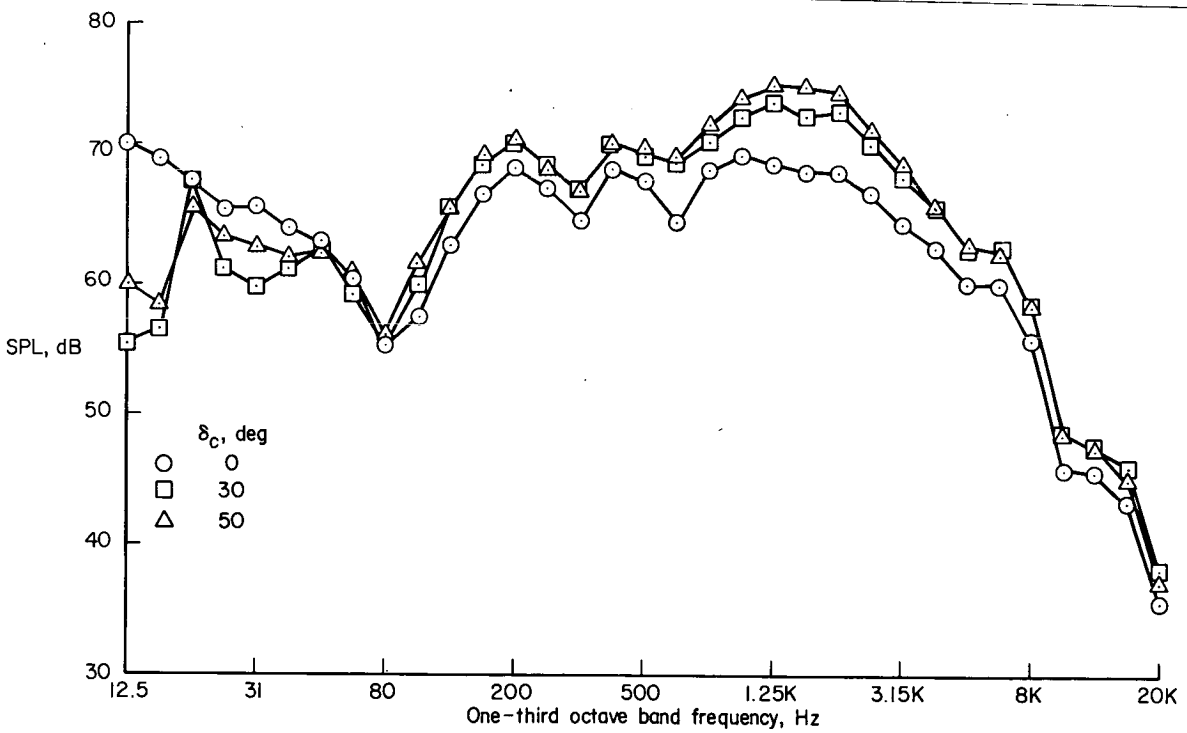

(c) Frequency spectra, U/W angle = 54°, $V_\infty = 33.5$ m/sec (106 ft/sec).

Figure 15.– Continued.

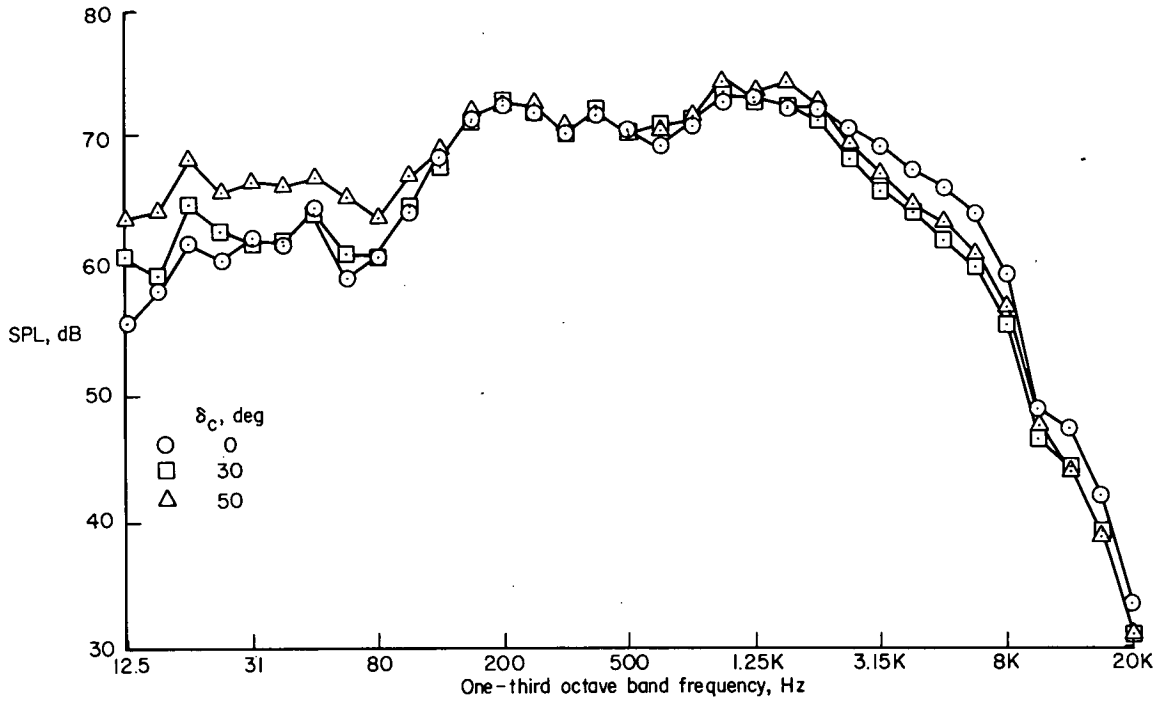

(d) Frequency spectra, U/W angle = 115°, V_∞ = 33.5 m/sec (106 ft/sec).

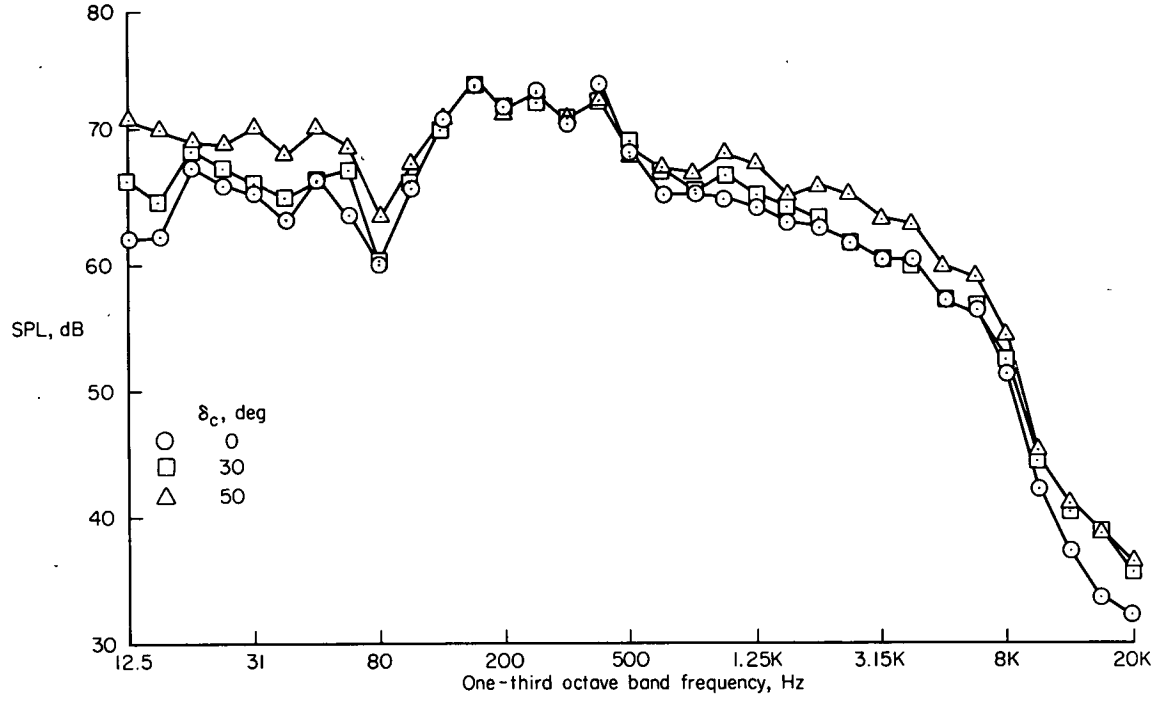

(e) Frequency spectra, U/W angle = 142°, V_∞ = 33.5 m/sec (106 ft/sec).

Figure 15.– Concluded.

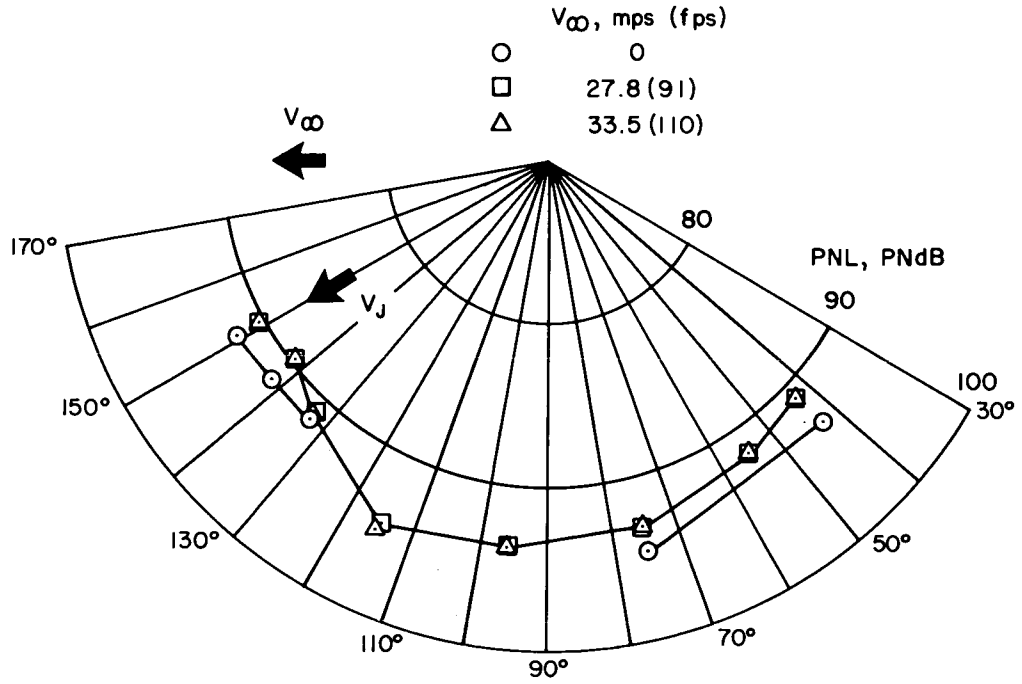

(a) *PNL* directivity, $\delta_f = \delta_a = 30°$, $V_{J_I} = 204$ m/sec (670 ft/sec), jet percent $b = 70$.

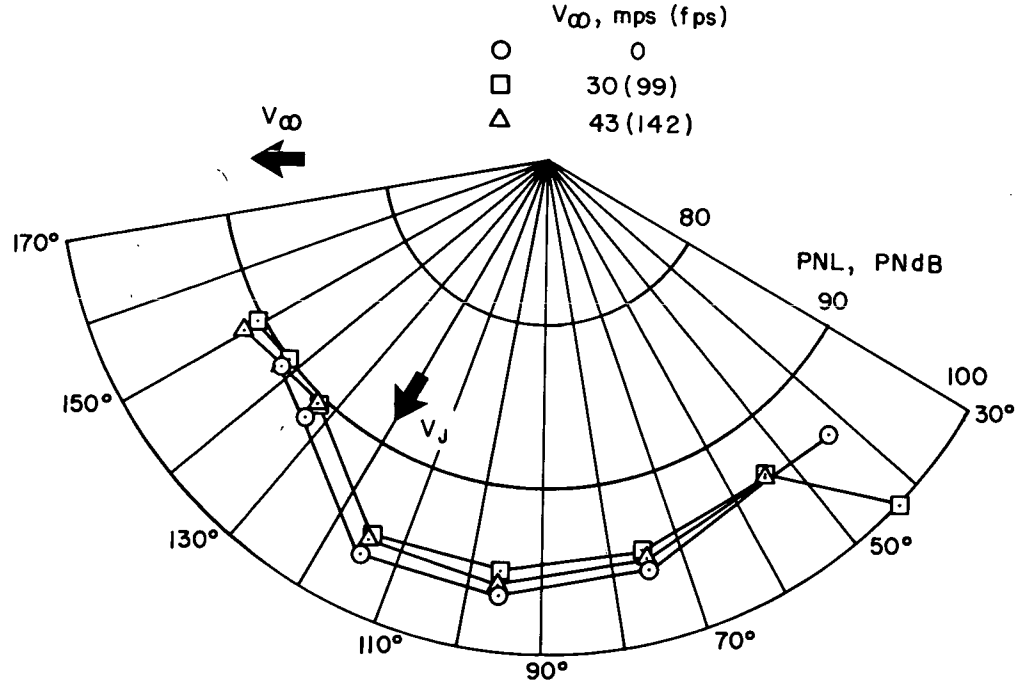

(b) *PNL* directivity, $\delta_f = \delta_a = 60°$, $V_{J_I} = 189$ m/sec (620 ft/sec), jet percent $b = 100$.

Figure 16.– Variation of underwing acoustic characteristics with forward speed; $\delta_c = 0°$, $\alpha = 0$.

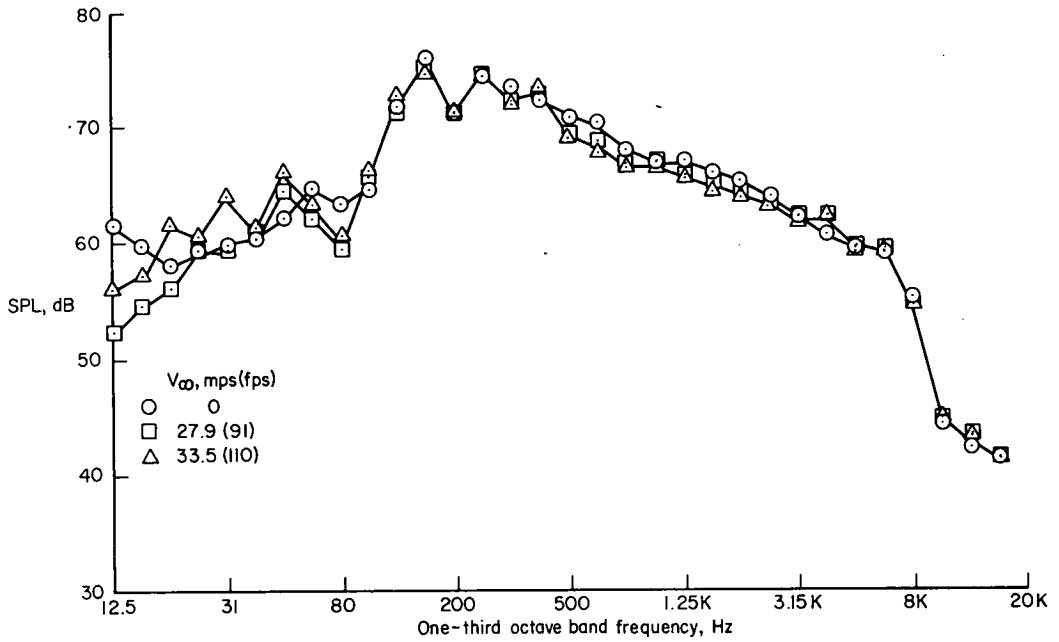

(c) Frequency spectra, U/W angle = 142°, $\delta_f = \delta_a = 30°$, $V_{J_I} = 204$ m/sec (670 ft/sec), jet percent $b = 70$.

Figure 16.– Concluded.

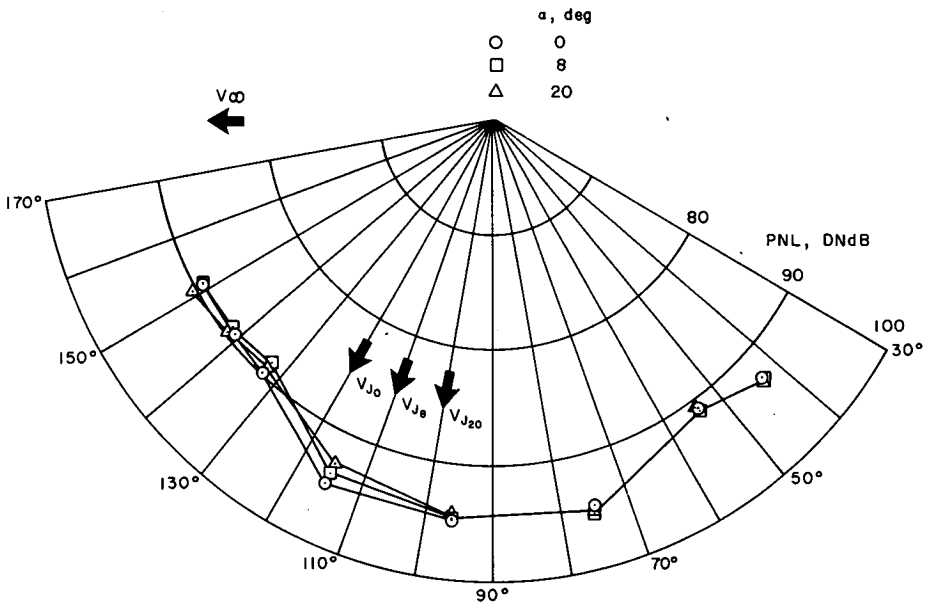

(a) *PNL* directivity, $\delta_f = 60°$, $\delta_c = 0°$, $\delta_a = 30°$, $V_{J_I} = 204$ m/sec (670 ft/sec), $V_\infty = 32.5$ m/sec (107 ft/sec), jet percent $b = 70$.

Figure 17.– Variation of underwing acoustic characteristics with angle of attack.

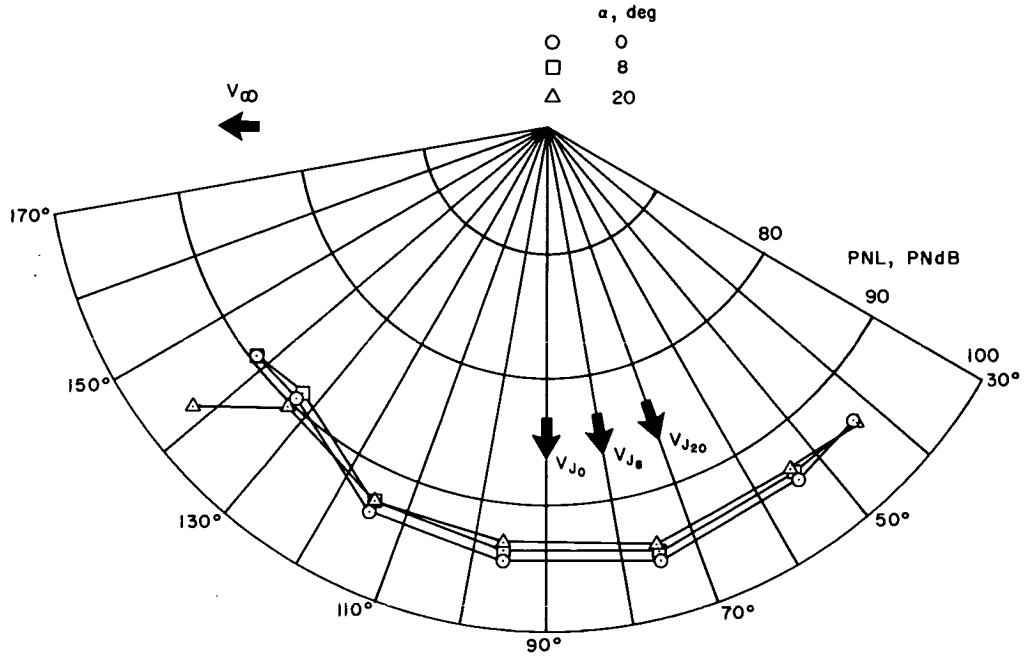

(b) *PNL* directivity, $\delta_f = 60°$, $\delta_c = 30°$, $\delta_a = 30°$, $V_{J_I} = 204$ m/sec (670 ft/sec), $V_\infty = 32.5$ m/sec (107 ft/sec), jet percent $b = 70$.

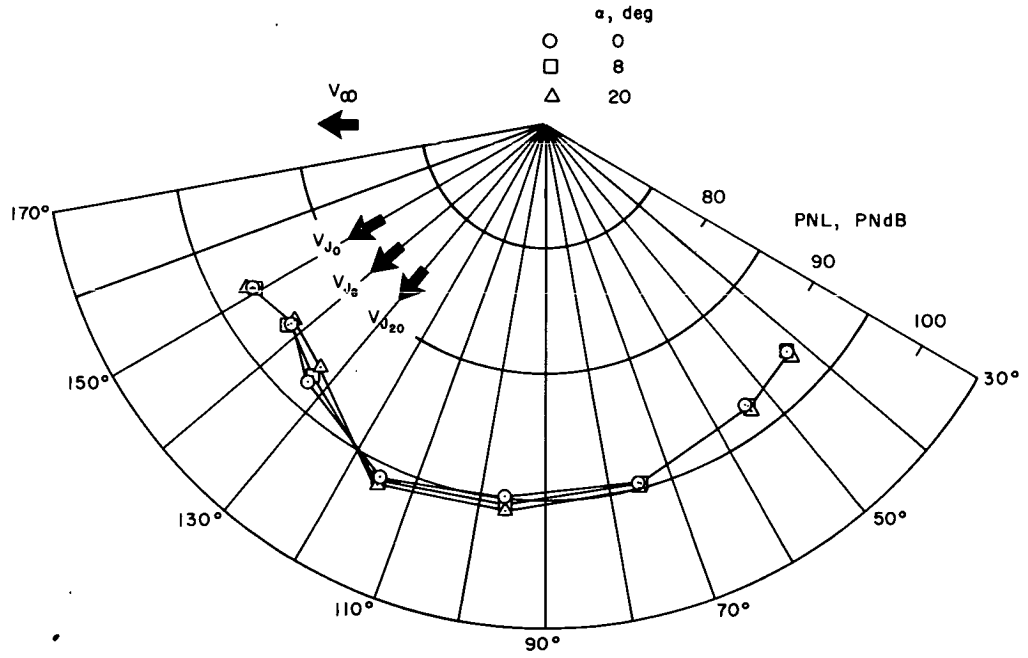

(c) *PNL* directivity, $\delta_f = \delta_a = 30°$, $\delta_c = 0°$, $V_{J_I} = 183$ m/sec (600 ft/sec), $V_\infty = 28.5$ m/sec (93.5 ft/sec), jet percent $b = 100$.

Figure 17.– Continued.

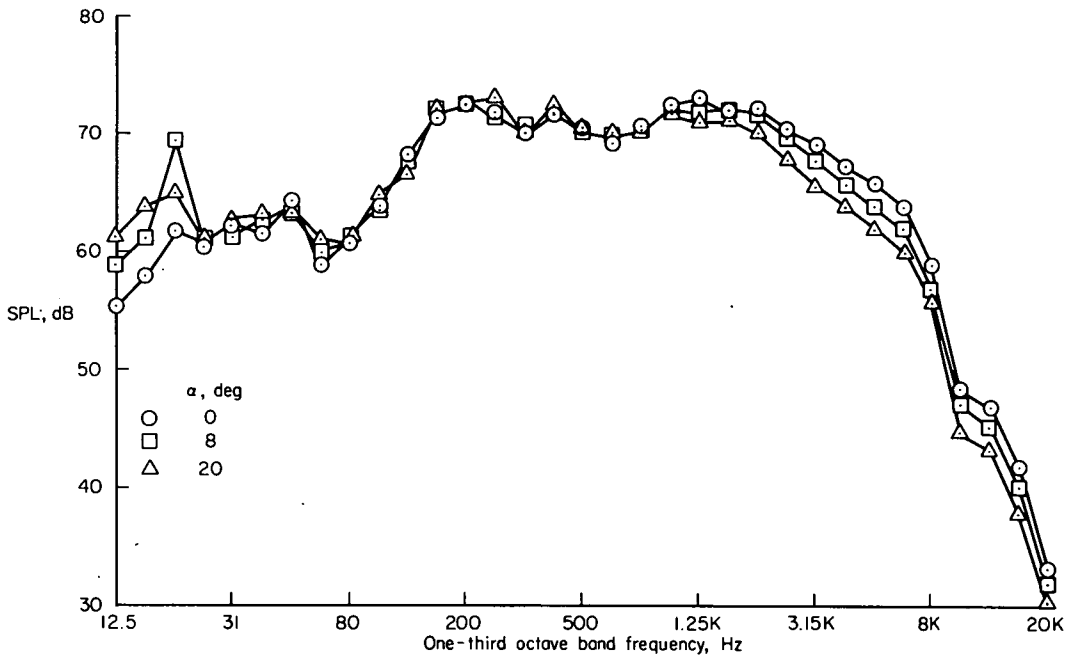

(d) Frequency spectra, U/W angle = 115°, δ_f = 60°, δ_c = 0°, δ_a = 30°, V_{J_I} = 204 m/sec (670 ft/sec), V_∞ = 32.5 m/sec (107 ft/sec), jet percent b = 70.

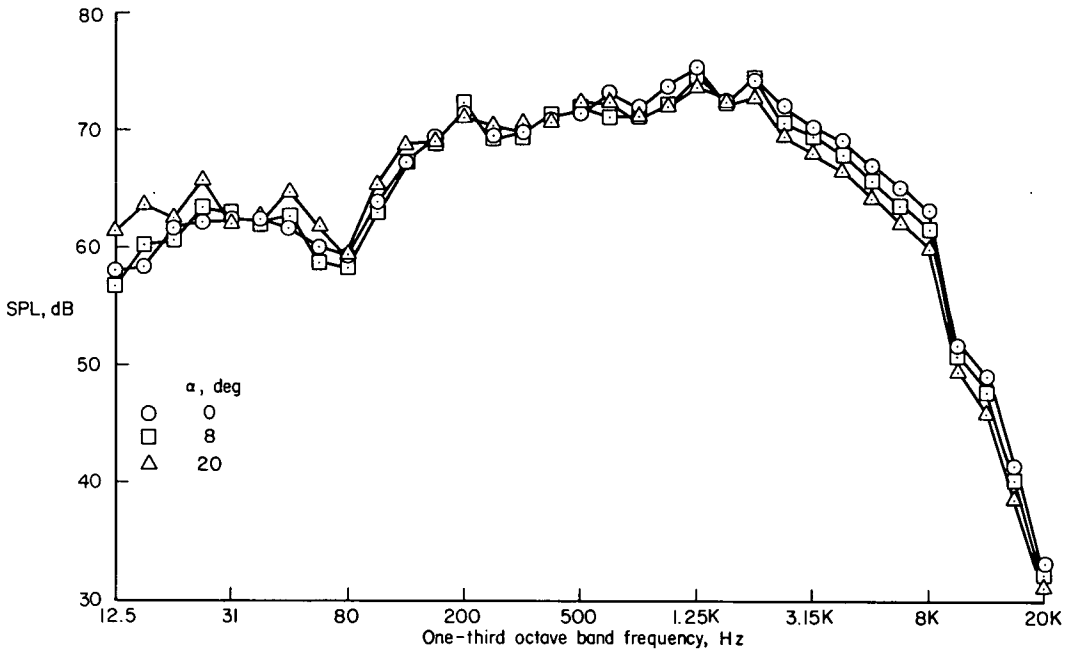

(e) Frequency spectra, U/W angle = 75°, δ_f = 60°, δ_c = 50°, δ_a = 30°, V_{J_I} = 204 m/sec (670 ft/sec), V_∞ = 32.5 m/sec (107 ft/sec), jet percent b = 70.

Figure 17.– Concluded.

NATIONAL AERONAUTICS AND SPACE ADMINISTRATION
WASHINGTON, D.C. 20546

OFFICIAL BUSINESS
PENALTY FOR PRIVATE USE $300

SPECIAL FOURTH-CLASS RATE
BOOK

POSTAGE AND FEES PAID
NATIONAL AERONAUTICS AND
SPACE ADMINISTRATION
451

U.S.MAIL

POSTMASTER : If Undeliverable (Section 158 Postal Manual) Do Not Return

"The aeronautical and space activities of the United States shall be conducted so as to contribute . . . to the expansion of human knowledge of phenomena in the atmosphere and space. The Administration shall provide for the widest practicable and appropriate dissemination of information concerning its activities and the results thereof."

—NATIONAL AERONAUTICS AND SPACE ACT OF 1958

NASA SCIENTIFIC AND TECHNICAL PUBLICATIONS

TECHNICAL REPORTS: Scientific and technical information considered important, complete, and a lasting contribution to existing knowledge.

TECHNICAL NOTES: Information less broad in scope but nevertheless of importance as a contribution to existing knowledge.

TECHNICAL MEMORANDUMS: Information receiving limited distribution because of preliminary data, security classification, or other reasons. Also includes conference proceedings with either limited or unlimited distribution.

CONTRACTOR REPORTS: Scientific and technical information generated under a NASA contract or grant and considered an important contribution to existing knowledge.

TECHNICAL TRANSLATIONS: Information published in a foreign language considered to merit NASA distribution in English.

SPECIAL PUBLICATIONS: Information derived from or of value to NASA activities. Publications include final reports of major projects, monographs, data compilations, handbooks, sourcebooks, and special bibliographies.

TECHNOLOGY UTILIZATION PUBLICATIONS: Information on technology used by NASA that may be of particular interest in commercial and other non-aerospace applications. Publications include Tech Briefs, Technology Utilization Reports and Technology Surveys.

Details on the availability of these publications may be obtained from:

SCIENTIFIC AND TECHNICAL INFORMATION OFFICE

NATIONAL AERONAUTICS AND SPACE ADMINISTRATION

Washington, D.C. 20546